Research Fund for the Control of Infectious Diseases

Research Dissemination Reports

控制傳染病研究基金

研究成果報告

Respiratory infectious diseases
呼吸道傳染病

Vector-borne diseases
病媒傳播疾病

Research Fund for the Control of Infectious Diseases

Research Dissemination Reports

VECTOR-BORNE DISEASES

Editorial

Dissemination reports are concise informative reports of health-related research supported by funds administered by the Food and Health Bureau, namely the *Research Fund for the Control of Infectious Diseases*. In this edition, 12 dissemination reports of projects related to respiratory infectious diseases and vector-borne diseases are presented. In particular, three projects are highlighted due to their potentially significant findings, impact on healthcare delivery and practice, and/or contribution to health policy formulation in Hong Kong.

Infectious disease is one of the leading causes of morbidity and hospitalisation in Hong Kong children over one year of age. The protective effect of breastfeeding against infectious diseases during infancy has been well documented. Tarrant et al[1] prospectively examined the impact of breastfeeding on hospitalisation secondary to infectious diseases up until 8 years of age in a large, well-established Hong Kong Chinese birth cohort, the "Children of 1997". The investigators found that breastfeeding for any duration substantially reduced hospitalisation for respiratory infections in infants aged 0 to 6 months. In addition, exclusive breastfeeding for 3 months or longer substantially reduced hospitalisation from gastrointestinal infections in infants aged 0 to 6 months. However, breastfeeding did not provide any long-term protective effect against hospitalisation secondary to infectious diseases in children.

Respiratory failure is the major complication in patients hospitalised with severe influenza A infection, and many patients progress rapidly to acute respiratory distress syndrome (ARDS) and multi-organ failure requiring intensive care support. Non-invasive positive pressure ventilation (NPPV) may play a limited supportive role for early ARDS/acute lung injury as a bridge to invasive mechanical ventilation during an influenza pandemic. However, the application of NPPV or other respiratory therapy may disperse potentially infected aerosols and contribute to nosocomial transmission of influenza. Hui et al[2] examined the directions and dispersion distances of exhaled air during application of common respiratory therapies such as oxygen masks, jet nebuliser, and NPPV via Respironics facemasks in a high-fidelity human patient simulator. The investigators found that substantial exposure to exhaled air occurs within 1 m from patients receiving NPPV. The authors made several recommendations for reducing the risk of exposure to infectious aerosols.

Live poultry exposure among the Hong Kong population through live poultry purchases decreased by more than 60% between 2004 and 2006, principally due to the reduction of imports and to a lesser extent, reduced touching during purchases, possibly reflecting impacts of public health education messages. Fielding et al[3] assessed the impact of health policy on behaviour by extending earlier surveys of avian influenza risk perception and live poultry exposure. The investigators found that declines in buying live poultry were not matched by declines in touching when buying. Continued buying of live poultry was associated with declines in perceived likelihood of influenza A/H5N1 infection risk. Population levels of trust in government and media messages about influenza A/H5N1 were unchanged. The surprising finding of this study was the increase in reliance on informal information sources.

A research impact evaluation was conducted 2 years after the project end date for many studies reported in this supplement. Impact was reported through publications in peer reviewed journals, gain of additional qualifications for project team members, career advancement, additional research funding obtained, stimulation of other research groups to conduct related research, and impact on policy and health care practices through changes in behaviour of health care professionals and/or other decision makers.

We hope you will enjoy this selection of research dissemination reports. Electronic copies of these dissemination reports and the corresponding full reports can be downloaded individually from the Research Fund Secretariat website (http://www.fhb.gov.hk/grants). Researchers interested in the funds administered by the Food and Health Bureau also may visit the website for detailed information about application procedures.

Supplement co-editors

Dr Ivy Cheung
Chief Secretariat Executive
(Research Office)
Food and Health Bureau

Dr Richard A. Collins
Scientific Review Director
(Research Office)
Food and Health Bureau

References

1. Tarrant M, Schooling CM, Leung SL, Mak KH, Ho LM, Leung GM. Impact of breastfeeding on infectious disease hospitalisation: the Children of 1997 cohort. Hong Kong Med J 2014;20(Suppl 4):5-6.
2. Hui DS, Chan MT, Chow B. Aerosol dispersion during various respiratory therapies: a risk assessment model of nosocomial infection to health care workers. Hong Kong Med J 2014;20(Suppl 4):9-13.
3. Fielding R, Cowling BJ, Liao Q, Lam WW. Behavioural changes in relation to risk perception and prevention of avian and human influenza in Hong Kong, 2006 to 2010. Hong Kong Med J 2014;20(Suppl 4):26-28.

Impact of breastfeeding on infectious disease hospitalisation: the Children of 1997 cohort

M Tarrant *, CM Schooling, SLS Leung, KH Mak, LM Ho, GM Leung

KEY MESSAGES

1. Breastfeeding for any duration substantially reduces hospitalisation from respiratory infections in Hong Kong infants from 0 to 6 months of age.

2. Exclusive breastfeeding for 3 months or longer substantially reduces hospitalisation from gastrointestinal infections in Hong Kong infants from 0 to 6 months of age.

3. Breastfeeding did not provide any long-term protective effect against infectious diseases hospitalisation in Hong Kong children.

[1] M Tarrant *, [2] CM Schooling, [3] SLS Leung, [4] KH Mak, [2] LM Ho, [1] GM Leung

[1] School of Nursing, The University of Hong Kong
[2] Department of Community Medicine, School of Public Health, The University of Hong Kong
[3] Family Health Service, Department of Health, Hong Kong SAR
[4] Student Health Service, Department of Health, Hong Kong SAR

* Principal applicant and corresponding author: tarrantm@hku.hk

Infectious disease is one of the leading causes of morbidity and hospitalisation in infants and young children. It is well established that breastfeeding substantially reduces the risk of infectious disease morbidity and mortality among this population. Breastfeeding may also have a long-term protective effect on resistance to infections. Although the exact mechanism is unclear, it is believed to be a result of human milk–mediated effects that produce a better functioning immune system in breastfed children. The World Health Organization recommends that infants be exclusively breastfed for 6 months with continued breastfeeding for up to 2 years of age and beyond.[1] This recommendation is based on the evidence that breastfed children grow up to be healthier and suffer lower rates of both infectious and chronic diseases. Although the breastfeeding rate in Hong Kong is increasing, it lags behind many other developed countries. The latest figures show that over 85% of Hong Kong mothers initiate breastfeeding, a 2.5% increase when compared with 2011.[2] However, few Hong Kong mothers breastfeed beyond the first few months and fewer still exclusively breastfeed for at least 6 months.

Hong Kong children achieve some of the best health outcomes in the developed world. Breastfeeding has been associated with reduced outpatient treatment rates for respiratory, gastrointestinal, and febrile illness in infants up to 18 months of age and reduced hospitalisation rates for respiratory illness in infants up to 9 months of age.[3] Data from the 'Children of 1997' cohort were examined to assess the benefits of breastfeeding among children up to 8 years of age.[4] All children in the cohort were born in Hong Kong in April and May of 1997. There were 8327 mother-infant pairs, accounting for 88% of all births during this period. Record linkage was used to link 97% of the birth cohort members to the Hospital Authority database.

The study reported that any amount of breastfeeding for ≥3 months reduced hospitalisation for respiratory, gastrointestinal, and any infections in infants aged 0 to 6 months; the reduction in hospitalisation was substantially greater with ≥3 months of exclusive breastfeeding.[4] Beyond 6 months of age, however, breastfeeding of any type did not provide protection from infectious disease hospitalisation. These findings suggest that the protective effect of breastfeeding is consistent with a direct stimulation of the infant's immune system through the transfer of antibodies and lymphocytes, and that breastfeeding does not provide a priming of the immune system that lasts substantially longer than the period of breastfeeding.

The protective effect of breastfeeding against infectious disease is dose-dependent, with a longer duration of exclusive breastfeeding conferring greater benefits.[5] Mothers should be encouraged and supported to breastfeed for a longer period and to meet the World Health Organization guidelines for 6 months of exclusive breastfeeding and continued breastfeeding for up to 2 year of age and beyond. Nonetheless, the challenge in Hong Kong is putting in place the mechanisms and supports to assist mothers to exclusively breastfeed for up to 6 months.

Acknowledgements

References

1. World Health Organization. Global strategy for infant and young child feeding. Geneva: World Health Organization; 2003.
2. Baby Friendly Hospital Initiative Hong Kong Association. World breastfeeding week 2013: annual summary. Hong Kong; 2013.
3. Leung GM, Lam TH, Ho LM, Lau YL. Health consequences of breast-feeding: doctors' visits and hospitalizations during the first 18 months of life in Hong Kong Chinese infants. Epidemiology 2005;16:328-35.
4. Tarrant M, Kwok MK, Lam TH, Leung GM, Schooling CM. Breast-feeding and childhood hospitalizations for infections. Epidemiology 2010;21:847-54.
5. Kramer MS, Kakuma R. The optimal duration of exclusive breastfeeding: a systematic review. Adv Exp Med Biol 2004;554:63-77.

Does chronic psychosocial stress modulate immunity to influenza vaccine in Hong Kong Chinese elderly?

SYS Wong *, J Woo, FWK Chan, CWK Lam, PKS Chan, CK Wong

KEY MESSAGES

1. The linear increase trend in the T-helper/suppressor ratio from 6 to 12 weeks was lower in elderly caregivers than non-caregivers (P=0.0041).

2. Caregivers had higher levels of inflammatory cytokine IL-6, which is an indicator of depression and poor health in older adults.

[1] SYS Wong *, [2] J Woo, [3] FWK Chan, [4] CWK Lam, [5] PKS Chan, [4] CK Wong

The Chinese University of Hong Kong:
[1] Department of Community and Family Medicine, School of Public Health
[2] Department of Medicine and Therapeutics
[3] School of Public Health
[4] Department of Chemical Pathology
[5] Department of Microbiology

* Principal applicant and corresponding author: yeungshanwong@cuhk.edu.hk

In the present study,[1] immune response to influenza vaccine of 55 elderly caregivers whose spouses were diagnosed with stroke, Parkinson's disease, or Alzheimer's disease and had severe limitation of activities of daily living was compared with that of 61 age- and sex-matched participants who did not have major caregiving responsibilities or whose spouses had no chronic condition. A commercially available trivalent influenza vaccine was given to all participants, and all blood samples were collected at similar time points. All participants were recruited from primary care institutes or the community, and all had received influenza vaccination in the previous year to standardise their most recent exposure to the vaccine. Validated scales were used to assess psychological (depressive symptoms, perceived stress and caregiver strain), social (multidimensional social support scale) and lifestyle (physical exercise, cigarette smoking, and alcohol consumption) parameters that have been documented to affect vaccine response.

At baseline, caregivers and non-caregivers did not differ significantly in terms of demographic and socio-economic factors. Caregivers spent a mean of 14 hours per day in caregiving and had higher perceived stress score, caregiver strain index score, and geriatric depression scale score, and lower total multidimensional social support scale score (family component), compared with non-caregivers. Caregivers also had less physical activity per week.

With regard to the antibody immune response to influenza vaccine, caregivers and non-caregivers did not differ significantly in terms of pre-vaccine immunity. In logistic regression analysis after adjusting for medical, psychological, and social factors, neither pre-vaccine status nor being a caregiver was related to post-vaccination antibody response.

Although there was no significant difference in immunophenotyping and enumeration of lymphocyte subsets at baseline, the linear increase trend in the T-helper/suppressor ratio from 6 to 12 weeks was lower in elderly caregivers than non-caregivers (P=0.0041).

With regard to the ex vivo production of pro-inflammatory cytokines (IL-10, IL-6, IL-8, IL-1 β, and IL-8), although caregivers had significantly higher levels at baseline, the increase in cytokines levels over 6 to 12 weeks was smaller, compared with non-caregivers, after adjusting for the geriatric depression scale score, education levels, physical activity, social support, smoking status, and body mass index.

Caregivers and non-caregivers did not differ significantly in terms of antibody response, but caregivers had a decrease in cell-mediated and cytokine immune response to influenza vaccination, even after adjusting for physical activity, body mass index, social support, and albumin level. This suggested that the mechanism responsible for the difference in cell-mediated response may not be related to health practice. People with caregiver stress appeared to have higher levels of ex vivo pro-inflammatory cytokine production.

Stress-related hormones (glucocorticoids and catecholamines) may play a role in the alteration of immune response.[2] Elderly caregivers may have poorer cell-mediated immune response, compared

to non-caregivers.[2] This is particularly relevant as ageing has an adverse impact on cell-mediated response to infections. Further studies are needed to determine whether being a caregiver is associated with decreased antibody response to influenza vaccination, as the present study had limited sample size and only included elderly subjects who had prior exposure to vaccination.

Acknowledgement

References

1. Wong SY, Wong CK, Chan FW, et al. Chronic psychosocial stress: does it modulate immunity to the influenza vaccine in Hong Kong Chinese elderly caregivers? Age (Dordr) 2013;35:1479–93.
2. Cohen S, Miller GE, Rabin BS. Psychological stress and antibody response to immunization: a critical review of the human literature. Psychosom Med 2001;63:7-18.

Aerosol dispersion during various respiratory therapies: a risk assessment model of nosocomial infection to health care workers

DSC Hui *, MTV Chan, B Chow

KEY MESSAGES

1. Substantial exposure to exhaled air occurs within 1 m from patients receiving non-invasive positive pressure ventilation, even in an isolation room with negative pressure, with far more extensive leakage and room contamination via the Image 3 facemask that requires connection to the whisper swivel exhalation port, especially at higher inspiratory pressures.

2. For non-invasive ventilation, it is advisable to choose facemasks with predictable exhaled air directions and distances through the exhalation port without addition of the whisper swivel device.

3. To avoid wider distribution of exhaled air and substantial room contamination during non-invasive ventilation, high inspiratory pressures should not be used.

4. The maximum exhaled air distances during application of jet nebuliser and oxygen via nasal cannula, Venturi mask, and the non-rebreathing mask were about 0.8 m, 0.42 m, 0.4 m, and <0.1 m, respectively.

5. More extensive exhaled air dispersion and room contamination occurs during application of a jet nebuliser to patients with more severe lung injury. Use of alternative methods to deliver bronchodilators (eg meter-dose inhaler via an aerochamber or a spacer) is advised.

[1] DSC Hui *, [2] MTV Chan, [3] B Chow

The Chinese University of Hong Kong:
[1] Department of Medicine and Therapeutics
[2] Department of Anaesthesia and Intensive Care
[3] Department of Architecture

* Principal applicant and corresponding author: dschui@cuhk.edu.hk

Introduction

Respiratory failure is a major complication in patients with influenza A/H5N1 infection. Many patients progress rapidly to acute respiratory distress syndrome (ARDS) and multi-organ failure, requiring intensive care support. Non-invasive positive pressure ventilation (NPPV) plays a supportive role for early ARDS/acute lung injury before resorting to invasive mechanical ventilation, although it is contra-indicated in critically ill patients with multi-organ failure and haemo-dynamic instability.[1] However, NPPV may disperse infected aerosols and lead to nosocomial transmission of influenza. Exhaled air particles can be dispersed up to 0.5 m from patients receiving NPPV using the Ultra Mirage mask (ResMed, Bella Vista, NSW, Australia).[2]

This study aimed to examine (1) the direction and dispersion distance of exhaled air particles during respiratory therapies such as the use of oxygen masks (nasal cannulae, simple masks, non-rebreathing), jet nebuliser, and NPPV via Respironics facemasks in a high-fidelity human-patient simulator (HPS), (2) the effectiveness of double-door negative pressure isolation room ventilation in minimising aerosol dispersion during these respiratory therapies, and (3) the effectiveness of double exhaust fans on the general medical ward in minimising aerosol dispersion when using a Venturi mask.

Methods

This study was conducted from February 2007 to January 2009. It received non-ionising radiation and biological/chemical safety approval by The Chinese University of Hong Kong. Except for testing the exhaled air dispersion distance from the Venturi mask on a general medical ward, the rest of the experiments were conducted in one of the 36, double-door, negative pressure (-5 Pa) isolation rooms measuring 2.8 x 4.22 x 2.4 m.

We studied the deliberate leakage from the exhalation ports of ComfortFull 2 and Image 3 masks (Respironics, Murrysville [PA], USA) and other respiratory therapies (jet nebuliser and various oxygen masks) firmly attached to a high-fidelity HPS (Medical Education Technologies, Sarasota [FL], USA). The HPS represented a 70-kg adult male sitting on a 45°-inclined hospital bed. The HPS was programmed to mimic different levels of severity of

TABLE. Maximum exhaled air dispersion distances during different respiratory therapies in the human-patient simulator (HPS) under different lung conditions

Respiratory therapy	Maximum exhaled air distance (m)
Non-invasive positive pressure ventilation	
ResMed Mirage mask (inspiratory/expiratory positive airway pressure, cmH$_2$O)*	
10/4	0.40
14/4	0.42
18/4	0.45
Respironics ComfortFull 2 mask (inspiratory/expiratory positive airway pressure, cmH$_2$O)*	
10/4	0.65
14/4	0.65
18/4	0.85
Respironics Image 3 mask plus whisper swivel exhalation valve (inspiratory/expiratory positive airway pressure, cmH$_2$O)*	
10/4	0.95
14/4	0.95
18/4	>0.95
Simple oxygen mask (oxygen flow, L/min)*	
4	0.20
6	0.22
8	0.30
10	0.40, >0.4 during coughing
Jet nebuliser (driven by air at 6 L/min)	
Normal lung	0.45
Mild lung injury	0.54
Severe lung injury	>0.80
Nasal cannula (oxygen flow, L/min)*	
1	0.30
1	0.25 (deflected upward when using electric blanket to mimic fever)
3	0.36
5	0.42
Venturi oxygen mask	
Normal lung	
24% oxygen	0.4
40% oxygen	0.33
Severe lung injury	
24% oxygen	0.32
40% oxygen	0.29
Non-rebreathing oxygen mask (oxygen flow, L/min)	
6, 8, 10, and 12	<0.1

* The HPS was programmed to mimic mild lung injury (lung compliance of 35 mL/cm H$_2$O and oxygen consumption of 300 mL/min). Tidal volume and respiratory rate were regulated so that a respiratory exchange ratio of 0.8 was maintained. Typically this was achieved with a tidal volume of 300 mL and a respiratory rate of 25 breaths/min

lung injury. Airflow was marked with intrapulmonary smoke for visualisation. A leakage jet plume was revealed by a laser-light sheet and images captured by high-definition video. Normalised exhaled air concentration in the plume was estimated from the light scattered by the smoke particles.[2-5] The normalised concentration contours were made up of data collected from at least 20 breaths. A contour value of 1 indicated a region that consisted entirely of air exhaled by the patient, where there was a very high chance of exposure to the exhaled air, such as at the mask exhaust vents. A value of 0 indicated no measurable air leakage in the region and a small chance of exposure to the exhaled air.[2-5]

Results

The exhaled air dispersion distances from various respiratory therapies are summarised in the Table.

Nasal cannula

The HPS was set in a mild lung injury mode (respiratory rate of 25/min and tidal volume of 300 mL). The dispersion distance of a low normalised concentration of exhaled smoke was 0.3 m along the sagittal plane from the mouth of the HPS at an oxygen flow rate of 1 L/min. When an electric blanket was wrapped around the HPS body to mimic fever, the exhaled plume was deflected slightly upward due to thermal buoyancy effect, and the radial distance was 0.25 m. When the oxygen flow was increased to 3 and 5 L/min without the electric blanket, the radial distance of low concentration of smoke increased to around 0.38 and 0.42 m, respectively, whereas more extensive room contamination with smoke was noted (Fig 1).

Jet nebuliser

The maximum dispersion distance of a low normalised concentration of smoke particles through the nebuliser side vent was 0.45 m lateral to the HPS at normal lung condition (oxygen consumption of 200 mL/min, lung compliance of 70 mL/cmH$_2$O). It increased to 0.54 m in mild lung injury (oxygen consumption of 300 mL/min, lung compliance of 35 mL/cmH2O), and beyond 0.8 m in severe lung injury (oxygen consumption of 500 mL/min, lung compliance of 10 mL/cmH2O). More extensive leakage through the side vents of the nebuliser mask was noted with more severe lung injury (Fig 2).[4]

Non-rebreathing mask

As oxygen was delivered at 6, 8, 10, and 12 L/min to the HPS with normal lung mechanics, the exhaled air dispersion distances of a low normalised concentration of smoke through the one-way exhalation valve ranged from 0.06 to 0.1 m, whereas those of a high normalised concentration of smoke

(a)

(b)
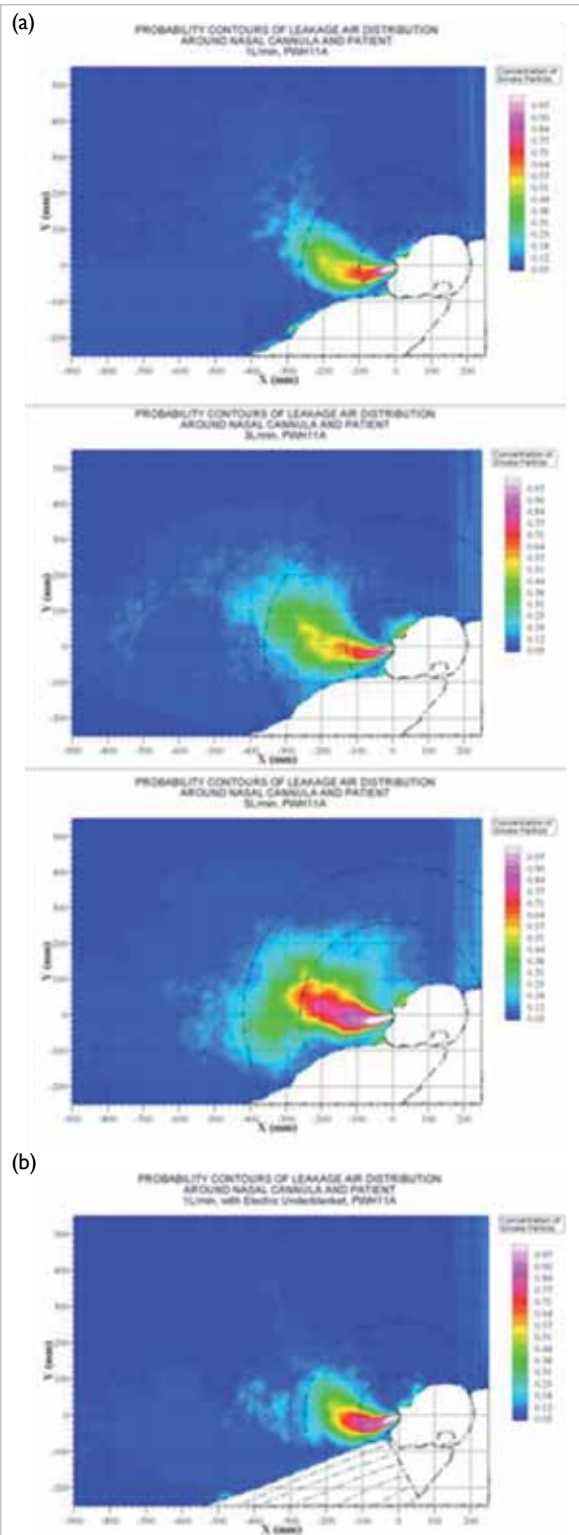
FIG 1. Exhaled air dispersion during application of oxygen via nasal cannulae

(a) When the oxygen flow was increased from 1 to 3 to 5 L/min, the radial distances of low normalised concentration of smoke were 0.3, 0.38, and 0.42 m from the human-patient simulator, respectively. (b) When an electric blanket was wrapped around the simulator body to mimic fever while receiving oxygen at 1 L/min, the exhaled plume was deflected slightly upward due to thermal buoyancy effect and the radial distance was 0.25 m.

(a)

(b)

(c)
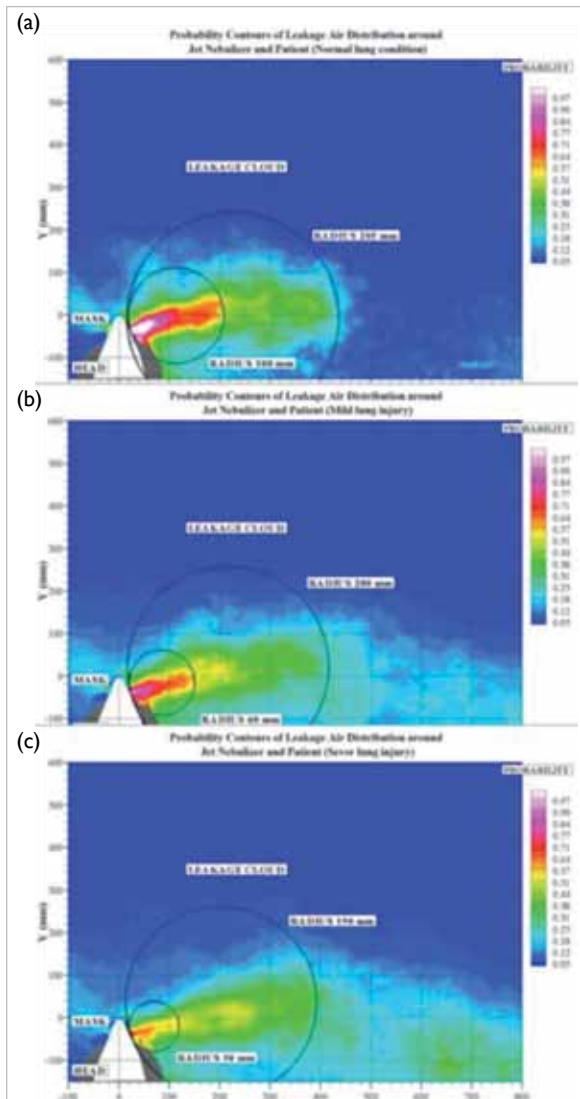
FIG 2. Exhaled air dispersion distances during application of a jet nebuliser were (a) 0.45 m, (b) 0.54 m, and (c) >0.8 m with the human-patient simulator programmed in conditions of normal lung, mild lung injury, and severe lung injury, respectively

ranged from 0.02 to 0.04 m. In severe lung injury mode, the exhaled air dispersion distances of a low normalised concentration of smoke ranged from 0.07 to 0.09 m, whereas those containing a high normalised concentration of smoke ranged from 0.02 to 0.04 m. The exhaled air distance was not proportional to the oxygen flow rate in either lung condition.

Venturi mask

In a general medical ward with double exhaust fans for room ventilation and HEPA filter, when 24% oxygen was delivered via a Venturi mask at 4 L/min to

the HPS with normal lung mechanics and then with severe lung injury, the exhaled air dispersion distances of a low normalised concentration of smoke through the exhalation port were 0.4 and 0.32 m, respectively, whereas those of a high normalised concentration of smoke were 0.17 and 0.14 m, respectively. When 40% oxygen was delivered at 8 L/min in the two lung conditions, the exhaled air dispersion distances of a low normalised concentration of smoke were 0.33 and 0.29 m, respectively, whereas those containing a high normalised concentration of smoke were the same at 0.14 m. Substantial exposure to exhaled air occurs within 0.4 m from patients receiving oxygen via a Venturi mask.

When the double exhaust fans were off, the air ventilation rates on the general medical ward dropped significantlly. The accumulative exhaled smokes filled up the ward within 5 minutes, and it was not technically feasible to measure the exhaled air dispersion distance from patients receiving oxygen via a Venturi mask.

Hudson mask with and without coughing

The HPS was programmed to breathe at a respiratory rate of 14 breaths/min and a tidal volume of 0.5 L. A jet plume of air leaked through the side vents of the simple oxygen mask to a lateral distance of 0.2, 0.22, 0.3, and 0.4 m from the sagittal plane during delivery of oxygen at 4, 6, 8, and 10 L/min, respectively. Coughing could extend the dispersion distance beyond 0.4 m. Substantial exposure to exhaled air occurs generally within 0.4 m from patients receiving supplemental oxygen via a simple mask.[3]

Non-invasive positive pressure ventilation

A bilevel positive airway pressure device (ResMed VPAP III ST, NSW, Australia) was used, and the expiratory positive airway pressure (EPAP) was maintained at 4 cmH_2O. When inspiratory positive airway pressure (IPAP) increased from 10 to 18 cmH_2O, the exhaled air of a low normalised concentration through the ComfortFull 2 mask increased from 0.65 to 0.85 m at a direction perpendicular to the head of the HPS along the median sagittal plane. In contrast, when an IPAP of 10 cmH_2O was applied via the Image 3 mask connected to the whisper swivel exhalation port, the exhaled air dispersed to 0.95 m towards the end of the bed along the median sagittal plane, whereas a higher IPAP resulted in wider spread of a higher concentration of smoke.[5]

The whisper swivel is an efficient exhalation device to prevent carbon dioxide rebreathing during NPPV, but it is not advisable in patients with febrile respiratory illness of unknown aetiology, especially during an influenza pandemic with high human-to-human transmission potential, for fear of major nosocomial infection. It is also important to avoid the use of higher IPAP, which could lead to wider distribution of exhaled air and substantial room contamination.[5]

Double-door negative pressure isolation room

Safe room environments depend on dilution and flow control toward extraction devices which target the exhaled air. This study confirmed the importance of maintaining adequate air ventilation rates in an isolation room—at least 12 air changes per hour—as recommended by the US Centers for Disease Control and World Health Organization. On the general medical ward, provision of double exhaust fans improved the air ventilation rates. Within isolation units, pressure differentials were essential for confining and removing exhaled air.

Discussion

In 2003, a nosocomial outbreak of SARS in our hospital was probably due to the use of a jet nebuliser for the administration of aerosolised albuterol in an index patient on a crowded medical ward. The maximum dispersion distance of exhaled air through the side vent of the jet nebuliser, driven by 6 L/min of air, was about 0.8 m lateral to the HPS.[4] The maximum exhaled air distances from patients receiving oxygen via a Hudson mask[3] and during NPPV via the ResMed mirage mask[2] were 0.4 and 0.5 m, respectively when the HPS was programmed at very mild lung injury. The maximum exhaled air distances from application of oxygen via nasal cannula, Venturi mask, and the non-rebreathing mask were 0.42, 0.4, and <0.1 m, respectively.

Our study was limited by the use of smoke particles as markers for exhaled air. The inertia and weight of larger droplets in an air-droplet two-phase flow would certainly cause them to have less horizontal dispersion than the continuous air carrier phase in which they travel due to increased inertia and drag. However, evaporation of water content in some droplets during NPPV and other respiratory therapies may produce droplet nuclei suspended in air, whereas the larger droplets fall to the ground in a trajectory pathway. As the smoke particles mark the continuous air phase, our data contours refer to exhaled air. Our results therefore represent the upper-bound estimates for the dispersion of droplets, which are expected to follow a shorter trajectory than the air jet due to gravitational effects, but they do not fully reflect the risk of droplet transmission.[2-5]

Substantial exposure to exhaled air occurred within 1 m from patients receiving NPPV in an isolation room with negative pressure via the ComfortFull 2 mask and the Image 3 mask connected to the whisper swivel exhalation port; the latter mask resulted in far more extensive leakage and

room contamination, especially at higher IPAP. The maximum exhaled air distances from application of jet nebuliser and oxygen via nasal cannula, Venturi mask, and the non-rebreathing mask were about 0.8, 0.42, 0.4, and <0.1 m, respectively. Health care workers should take adequate precautions when providing respiratory support to patients with pneumonia of unknown aetiology complicated by respiratory failure.

Acknowledgment

References

1. Hui DS. Influenza A/H5N1 infection: other treatment options and issues. Respirology 2008;13(Suppl 1):S22-6.
2. Hui DS, Hall SD, Chan MT, et al. Noninvasive positive-pressure ventilation: an experimental model to assess air and particle dispersion. Chest 2006;130:730-40.
3. Hui DS, Hall SD, Chan MT, et al. Exhaled air dispersion during oxygen delivery via a simple oxygen mask. Chest 2007;132:540-6.
4. Hui DS, Chow BK, Chu LC, et al. Exhaled air and aerosolized droplet dispersion during application of a jet nebulizer. Chest 2009;135:648-54.
5. Hui DS, Chow BK, NG SS, et al. Exhaled air dispersion distances during noninvasive ventilation via different Respironics face masks. Chest 2009;136:998-1005.

Cellular signalling pathways of matrix metalloproteinase gene expression by *Pseudomonas aeruginosa*–infected human bronchial epithelial cells

WS Hui, SP Ho, AT Wong, PL Ho, JCW Mak *

KEY MESSAGES

1. *Pseudomonas aeruginosa* infection is associated with increased production of matrix metalloproteinase-9 (MMP-9) from the airway epithelium; inappropriate expression and activation of MMP-9 may be associated with tissue injury and airway remodelling.

2. *P aeruginosa* exposure induces the phosphorylation of ERK, JNK, and p38 MAPKs in human airway epithelial cell line (BEAS-2B). Inhibition of ERK or JNK activity blocks IL-8 and MMP-9 mRNA and protein expression in BEAS-2B cells infected with *P aeruginosa*.

3. Induction of IL-8 and MMP-9 in human bronchial epithelial cells by *P aeruginosa* infection is mediated via the NF-κB-mediated pathway, possibly through upstream ERK and JNK MAPK pathways.

4. *P aeruginosa* infection initiates an intense inflammatory response, such as the release of IL-8, which progressively destroys pulmonary tissue via MMP-9 activation and is associated with high mortality.

5. Inhibition of ERK or JNK may be an effective therapeutic strategy against the early stages of pulmonary *P aeruginosa* infection, via attenuation of the inflammatory cascade.

[1] WS Hui, [1] SP Ho, [1] AT Wong, [2] PL Ho, [1] JCW Mak *

The University of Hong Kong:
[1] Division of Respiratory and Critical Care Medicine, Department of Medicine
[2] Department of Microbiology

* Principal applicant and corresponding author: judithmak@hku.hk

Introduction

Pseudomonas aeruginosa is a Gram-negative bacillus and an opportunistic pathogen that causes pneumonia in immunocompromised humans and severe pulmonary damage in non-cystic fibrosis bronchiectasis.[1] Because of the severity of *P aeruginosa* infection, it is important to understand the mechanisms of the resulting epithelial injury and repair processes during conditions of airway inflammation. *P aeruginosa* is a pathogen in chronic obstructive pulmonary disease associated with an intense airway inflammation and poor prognosis.[2,3] The initial step of bacterial infection, crucial for the development of permanent colonisation at later stages, is the adherence of the bacteria to epithelial cells. The infection is associated with an excessive inflammatory response, characterised by the accumulation of large amounts of the polymorphonuclear leukocyte chemokine IL-8 and its toxic products in the airways.[4]

The matrix metalloproteinases (MMPs) are a family of proteolytic enzymes that degrade the main protein components of extracellular matrices and may lead to continued airway obstruction when uncontrolled.[5] They are produced by structural cells such as fibroblasts and epithelial cells, and by many inflammatory cells including macrophages, eosinophils, neutrophils, and mast cells. They are secreted as latent proenzymes and are converted to the active form by proteolytic cleavage of an amino-terminal domain. The MMPs are important in tissue remodelling in the airways through their ability to affect the integrity of the basal lamina and the degree of infiltration by inflammatory cells. The balance between activated MMPs and the endogenous tissue inhibitor of metalloproteinases (TIMPs) determine overall MMP proteolytic activity, and thus the turnover of airway extracellular matrix. Several MMPs including MMP-9 play an important role in the pathogenesis of many airway diseases such as asthma and chronic obstructive pulmonary disease.[6,7] An up-regulation of MMP-8 and -9 has been reported in human bronchiectatic airways in vivo.[8] Furthermore, MMP-2 and -9 expression is increased in mouse mycoplasma-infected airways in vivo.[9]

Studies have shown that mitogen-activated protein kinases (MAPKs) are involved in the

regulation of MMPs by various cell types.[10,11] The MAPK family includes three major members: the extracellular signal-regulated kinases (ERKs), the c-Jun N-terminal kinase (JNK)/stress-activated protein kinases, and p38.[12] Although the role of MAPKs in the regulation of MMPs has been studied in many cell types, little is known about how MAPKs regulate the production of MMPs after bacterial infection in airway epithelial cells. We hypothesised that *P aeruginosa* infection induces MMP-9 in human bronchial epithelial cells via NF-κB activation. As NF-κB is a candidate for therapeutic intervention in airway inflammation, we also investigated the role of NF-κB in the induction of MMP-9 expression after *P aeruginosa* infection.

We investigated the expression and activity of MMP-9 in human bronchial epithelial cells using RT-PCR and gelatin zymography. The role of specific MAPK pathways in the activation of NF-κB-dependent transcription was addressed using NF-κB-dependent transcriptional reporters (ie BEAS-2B 6κBtk reporter cell line) and specific MAPK inhibitors.

Methods

Cell culture and *Pseudomonas aeruginosa* infection

BEAS-2B cells were grown in Keratinocyte-SFM containing 5 ng/ml epidermal growth factor and 50 µg/ml bovine pituitary extract, and then incubated at 37ºC in a humidified incubator with 95% air and 5% CO_2. Passages 41-49 were used. At 90% confluence, the culture was changed to growth factor-free medium for 24 h prior to treatment.

Different *P aeruginosa* strains (one clinical isolate from a local patient, PAO1 as a laboratory strain [ATCC15692] and ATCC27853 as a reference strain) were used at 10^7 to 10^5 colony-forming units for various time periods.

Semi-quantitative RT-PCR

Total cDNA was prepared by first-strand cDNA synthesis from 1 µg of total RNA isolated from cells according to standard protocols. For PCR quantification, appropriate primers for IL-8, MMPs (MMP-2, MMP-8, and MMP-9) and TIMPs (TIMP-1 and TIMP-2) were designed according to the published sequences. Following amplification, PCR products were run on an ethidium bromide-stained agarose gel. Bands were quantified by densitometric analysis using glyceraldehydes-3-phosphate-dehydrogenase (GAPDH) as a housekeeping gene. Data were expressed as the ratio of gene of interest/GAPDH.

ELISA

IL-8 was measured in the supernatant using commercially available ELISA kits (BD OptEIASet).

Gelatine zymography

Levels of gelatinolytic MMPs, secreted into the media, were separated by electrophoresis through a 10% polyacrylamide gel containing 0.1% gelatine. Positions of gelatinolytic activity were unstained on a darkly stained background. The clear bands on the zymograms were scanned and the signals quantified by densitometric scanning to determine the intensity of MMP-9 activity as arbitrary units.

Western blot analysis

After infection with *P aeruginosa*, protein was extracted from cells. Samples (20 µg) were run on 10% on SDS-polyacrylamide gels with prestained molecular weight markers (Bio-Rad) and transferred to Hybond-ECL membranes using standard techniques. Membranes were blocked with 5% nonfat milk and probed with primary antibodies to phosphorylated or total ERK1/2, JNK1/2 and p38 (Cell Signaling Technology) at a dilution of 1:1000 and incubated overnight at 4ºC. HRP-conjugated goat anti-rabbit or anti-mouse antibody was used as a secondary antibody. In all cases, proteins were visualised using enhanced chemiluminescence reagent (Amersham) according to the manufacturer's instructions.

Luciferase activity assay

The BEAS-2B 6κBtk reporter cell line was generated as described previously.[13] Luciferase activity was determined using a commercially available luciferase reporter gene assay system (Promega) under luminescence (FLUOstar Plate Reader).

Statistical Analysis

Values were expressed as means±SEM. Data analysis was performed using Prism software (GraphPad Software). All experiments were carried out with materials collected from at least four to six separate cell cultures in duplicate or triplicate. Comparison of more than two groups was carried out with one-way analysis of variance, followed by Bonferroni's multiple comparison post hoc tests. A P value of <0.05 was considered statistically significant.

Results

P aeruginosa–induced IL-8 was released in a dose- and time-dependent manner. As the three different strains of *P aeruginosa* released comparable amount of IL-8, PAO1 was chosen for further study. Induction of IL-8 mRNA expression appeared as early as 1 h after exposure to *P aeruginosa* (preceding the release of IL-8) and continued to increase for up to 4 h.

Cells were found to express MMP-2 and MMP-9, which were secreted in their proforms
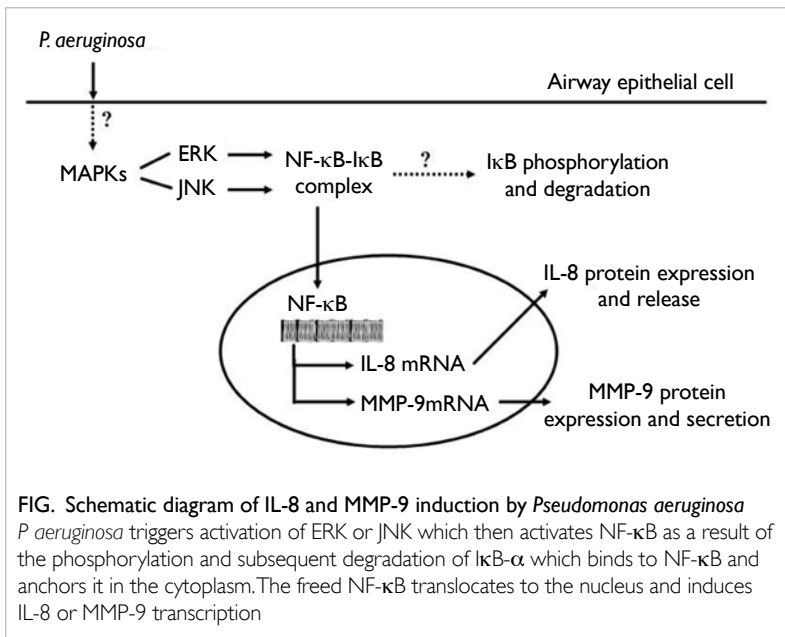
FIG. Schematic diagram of IL-8 and MMP-9 induction by *Pseudomonas aeruginosa*
P aeruginosa triggers activation of ERK or JNK which then activates NF-κB as a result of the phosphorylation and subsequent degradation of IκB-α which binds to NF-κB and anchors it in the cytoplasm. The freed NF-κB translocates to the nucleus and induces IL-8 or MMP-9 transcription

(proMMP; MMP-2 proform, 72 kD; MMP-9 proform, 92 kD). *P aeruginosa* caused a dose-dependent increase in MMP-9 production, but the MMP-2 was not affected after 6h. Induction of MMP-9 mRNA expression was detectable at 1 h and reached plateau at 2 h after infection, indicating transcriptional regulation.

Although phosphorylation of the MAPKs ERK, JNK, and p38 at Thr^{202}/Tyr^{204}, Thr^{183}/Tyr^{185}, and Thr180/Tyr182 was detectable at 1 h and continued to increase up to 2 h after *P aeruginosa* exposure. The MEK and JNK activity inhibitors, PD98059 and SP600125 respectively, blunted IL-8 release and MMP-9 activity in BEAS-2B cells treated with *P aeruginosa* but not p38 MAPK inhibitor SB203580. The *P aeruginosa*–induced IL-8 mRNA also diminished in the presence of PD98059 and SP600125 but not SB203580, suggesting that *P aeruginosa*–induced ERK and JNK activity partially contributed to *P aeruginosa*–induced IL-8 release and MMP-9 activity in BEAS-2B cells.

Treatment with pyrrolidine dithiocarbamate (a NF-κB inhibitor) before *P aeruginosa* infection attenuated *P aeruginosa*–induced IL-8 release and MMP-9 activity. *P aeruginosa* (either PAO1 or a clinical isolate) alone caused a dose-dependent increase in NF-κB-dependent transcription, which was diminished at ≥10 μM for PD98059 and SP600125.

Discussion

The enzymes of MMP family are important in tissue development and regeneration. Inappropriate MMP regulation and activation during chronic inflammation may lead to disturbances in the turnover and remodelling of pulmonary extracellular matrix, which could contribute to the structural remodelling that occurs after bacterial infection. In the present study, *P aeruginosa* infection induced the expressions of IL-8 and MMP-9, the pivotal inflammatory mediators through a mechanism that involved ERK1, JNK, and NF-κB activation in BEAS-2B cells.

Lung epithelial cells can be activated directly by some microbes, such as *P aeruginosa*.[14] A variety of cellular signalling pathways can be altered by acute lower respiratory tract infection including MAPK signalling and NF-κB activation, among others.[15] The MPPKs are important transducers of extracellular stimuli to the nucleus. The mechanisms of MAPK-mediated gene expression include the modulation of transcription factor activity.[16] NF-κB is also an important transcription factor activating the IL-8 promoter.[17] In support of NF-κB involvement, *P aeruginosa* infection induced the activity of a reporter construct governed by a 6x tandem repeat of the NF-κB response element in BEAS-2B cells, suggesting that NF-κB might be involved in *P aeruginosa*–induced IL-8 and MMP-9 promoter activity.

To our knowledge, there is no study addressing the significance of ERK and JNK signalling after *P aeruginosa* infection. In accordance with our findings, ERK has been linked to production of MMP-9, and to IL-8 release in response to lipopolysaccharide or *Helicobacter pylori* through in vitro studies of primary monocytes and macrophage cell lines.[18,19] The present study indicated that inhibition of ERK or JNK suppressed *P aeruginosa*–induced increases in the luciferase activity of an NF-κB-dependent reporter, supporting the possibility of the role of ERK or JNK as an upstream activator of NF-κB. An ERK- or JNK-NF-κB-linked cascade was important in the case of human airway epithelial cells (Fig). We therefore suggest that inhibition of ERK or JNK may be an effective therapeutic strategy against the early stages of pulmonary *P aeruginosa* infection, via attenuation of the inflammatory cascade.

Acknowledgement

References

1. Ho PL, Chan KN, Ip MS, et al. The effect of *Pseudomonas aeruginosa* infection on clinical parameters in steady-state bronchiectasis. Chest 1998;114:1594-8.
2. Lin SH, Kuo PH, Hsueh PR, Yang PC, Kuo SH. Sputum bacteriology in hospitalized patients with acute exacerbation of chronic obstructive pulmonary disease in Taiwan with an emphasis on *Klebsiella pneumoniae* and

Pseudomonas aeruginosa. Respirology 2007;12:81-7.

3. Murphy TF, Brauer AL, Eschberger K, et al. *Pseudomonas aeruginosa* in chronic obstructive pulmonary disease. Am J Respir Crit Care Med 2008;177:853-60.

4. Tsang KW, Ho PL, Lam WK, et al. Inhaled fluticasone reduces sputum inflammatory indices in severe bronchiectasis. Am J Respir Crit Care Med 1998;158:723-7.

5. Parks WC, Shaprio SD. Matrix metalloproteinases in lung biology. Respir Res 2001;2:10-9.

6. Hoshino M, Nakamura Y, Sim J, Shimojo J, Isogai S. Bronchial subepithelial fibrosis and expression of matrix metalloproteinase-9 in asthmatic airway inflammation. J Allergy Clin Immunol 1998;102:783-8.

7. Vignola AM, Riccobono L, Mirabella A, et al. Sputum metalloproteinase-9/tissue inhibitor of metalloproteinase-1 ratio correlates with airflow obstruction in asthma and chronic bronchitis. Am J Respir Crit Care Med 1998;158:1945-50.

8. Zheng L, Lam WK, Tipoe GL, et al. Overexpression of matrix metalloproteinase-8 and -9 in bronchiectatic airways in vivo. Eur Respir J 2002;20:170-6.

9. Baluk P, Raymond WW, Ator E, Coussens LM, McDonald DM, Caughey GH. Matrix metalloproteinase-2 and -9 expression increases in Mycoplasma-infected airways but is not required for microvascular remodeling. Am J Physiol Lung Cell Mol Physiol 2004;287:L307-17.

10. Reunanen N, Westermarck J, Hakkinen L, et al. Enhancement of fibroblast collagenase (matrix metalloproteinase-1) gene expression by ceramide is mediated by extracellular signal-regulated and stress-activated protein kinase pathways. J Biol Chem 1998;273:5137-45.

11. McCawley LJ, Li S, Wattenberg EV, Hudson LG. Sustained activation of the mitogen-activated protein kinase pathway. A mechanism underlying receptor tyrosine kinase specificity for matrix metalloproteinase-9 induction and cell migration. J Biol Chem 1999;274:4347-53.

12. Kyriakis JM, Avruch J. Mammalian mitogen-activated protein kinase signal transduction pathways activated by stress and inflammation. Physiol Rev 2001;81:807-69.

13. Catley MC, Cambridge LM, Nasuhara Y, et al. Inhibitors of protein kinase C (PKC) prevent activated transcription: role of events downstream of NF-kappaB DNA binding. J Biol Chem 2004;279:18457-66.

14. Soong G, Reddy B, Sokol S, Adamo R, Prince A. TLR2 is mobilized into an apical lipid raft receptor complex to signal infection in airway epithelial cells. J Clin Invest 2004;113:1482-9.

15. Mizgerd JP. Acute lower respiratory tract infection. N Engl J Med 2008;358:716-27.

16. Hill CS, Treisman R. Transcriptional regulation by extracellular signals: mechanisms and specificity. Cell 1995;80:199-211.

17. Roebuck KA. Regulation of interleukin-8 gene expression. J Interferon Cytokine Res 1999;19:429-38.

18. Bhattacharyya A, Pathak S, Datta S, Chattopadhyay S, Basu J, Kundu M. Mitogen-activated protein kinases and nuclear factor-kappaB regulate Helicobacter pylori-mediated interleukin-8 release from macrophages. Biochem J 2002;368:121-9.

19. Lai WC, Zhou M, Shankavaram U, Peng G, Wahl LM. Differential regulation of lipopolysaccharide-induced monocyte matrix metalloproteinase (MMP)-1 and MMP-9 by p38 and extracellular signal-regulated kinase 1/2 mitogen-activated protein kinases. J Immunol 2003;170:6244-9.

Substrate specificity and rational design of peptidomimetic inhibitors for SARS coronavirus main protease

KB Wong *, DCC Wan, HF Chow

KEY MESSAGES

1. Substrate-specificity of the main protease of SARS coronavirus was systematically profiled at P5 to P3' positions, which provided insights into a rational design of peptidomimetic inhibitors.

2. Leu and Gln were most favoured at P2 and P1 positions, respectively. Substrate preferences at P5 to P3 positions were important in enhancing the main protease activity. 'Super-reactive' substrate sequences were engineered, with more than a 2-fold increase in activity, by combining the best residue choices at P5 to P3 positions.

3. A novel class of peptidomimetic inhibitor against the main protease was developed using the nitrile warhead. The most potent inhibitor synthesised was Cbz-AVLQ-CN, with an IC50 value of 5 µM.

4. The crystal structure of the main protease in complex with Cbz-AVLQ-CN was determined, which provided structural insights into protease-inhibitor interactions for future structured-basis design of inhibitors.

[1] KB Wong *, [2] DCC Wan, [3] HF Chow

[1] School of Life Sciences, The Chinese University of Hong Kong
[2] School of Biomedical Sciences, The Chinese University of Hong Kong
[3] Department of Chemistry, The Chinese University of Hong Kong

* Principal applicant and corresponding author: kbwong@cuhk.edu.hk

The main protease (M^{pro}) of severe acute respiratory syndrome coronavirus (SARS CoV) is a key enzyme for viral replication, and is thus an attractive target for anti-SARS CoV drug development. M^{pro} belongs to the family of 3C-like cysteine proteases. The basic design of peptidomimetic inhibitors involved a warhead that can form covalent modifications to the –SH group of the active site residue Cys145 and a substrate peptide sequence that forms favourable interactions with the protease.

We systematically profiled the substrate specificity of M^{pro}, which forms the basis of a rational design of peptidomimetic inhibitors.[1] First, we created a library of protein-based substrates, and profiled the preference of amino acid residues at each of the P5 to P3' positions. Based on the substrate-specificity profile, we created 'super-reactive' substrate sequences. In addition, a novel peptidomimetic inhibitor was synthesised using nitrile as the warhead.[2] A number of inhibitors were synthesised to test the role of N-terminal protective groups and the substrate peptide sequences. Finally, the crystal structure of M^{pro} in complex with the best inhibitor was determined to provide a better understanding of protease-inhibitor interactions.

The results on substrate specificity profile of M^{pro} have been reported.[1] To profile the substrate-specificity of the SARS-CoV M^{pro}, saturated mutagenesis was performed at each of the P5 to P3' positions of the WT auto-cleavage sequences (SAVLQ↓SGF) [Fig 1]. A library of 19x8 variant substrate sequences was created and their relative activity was measured. At the P5 position, many substitutions exhibited higher activity than the WT substrate. The most preferred residue at the P5 position was Val. At the P4 position, small residues (Ala, Cys, Ser, Val, and Thr) were favoured. Substitutions with a bulky residue (Phe, Trp, Tyr, Leu, Met), or large polar residues (Lys, Arg, His, Asp, Glu, Asn) resulted in substrate sequences that had low relative activity. The best residue at the P4 position was Val. At the P3 position, positively charged residues (Lys, Arg) were favoured, but negatively charged residues (Glu, Asp) were repelled. The only non-cleavable substitution was V3P. The best residue this position was Arg. At the P2 position, only hydrophobic residues (Ala, Ile, Leu, Met, Phe, Pro, and Val) could be cleaved. The best residue was Leu. At the P1 position, the substrate sequence required a Gln residue to enable cleavage.[3-5] Surprisingly, M^{pro} was able to cleave substrate sequences containing a His or a Met. This finding challenges the established view that Gln is required at the P1 position. If M^{pro} can recognise His/Met at the P1 position, there may be more cleavage sites for M^{pro} along the SARS polyprotein. At the P1' position, small residues (Ala, Cys, Gly, and Ser) were favoured. Substitutions with large residues resulted in significant reduction in the relative activity. At the P2' position, small residues (Gly, Ala, Ser, and Thr) were also favoured, although
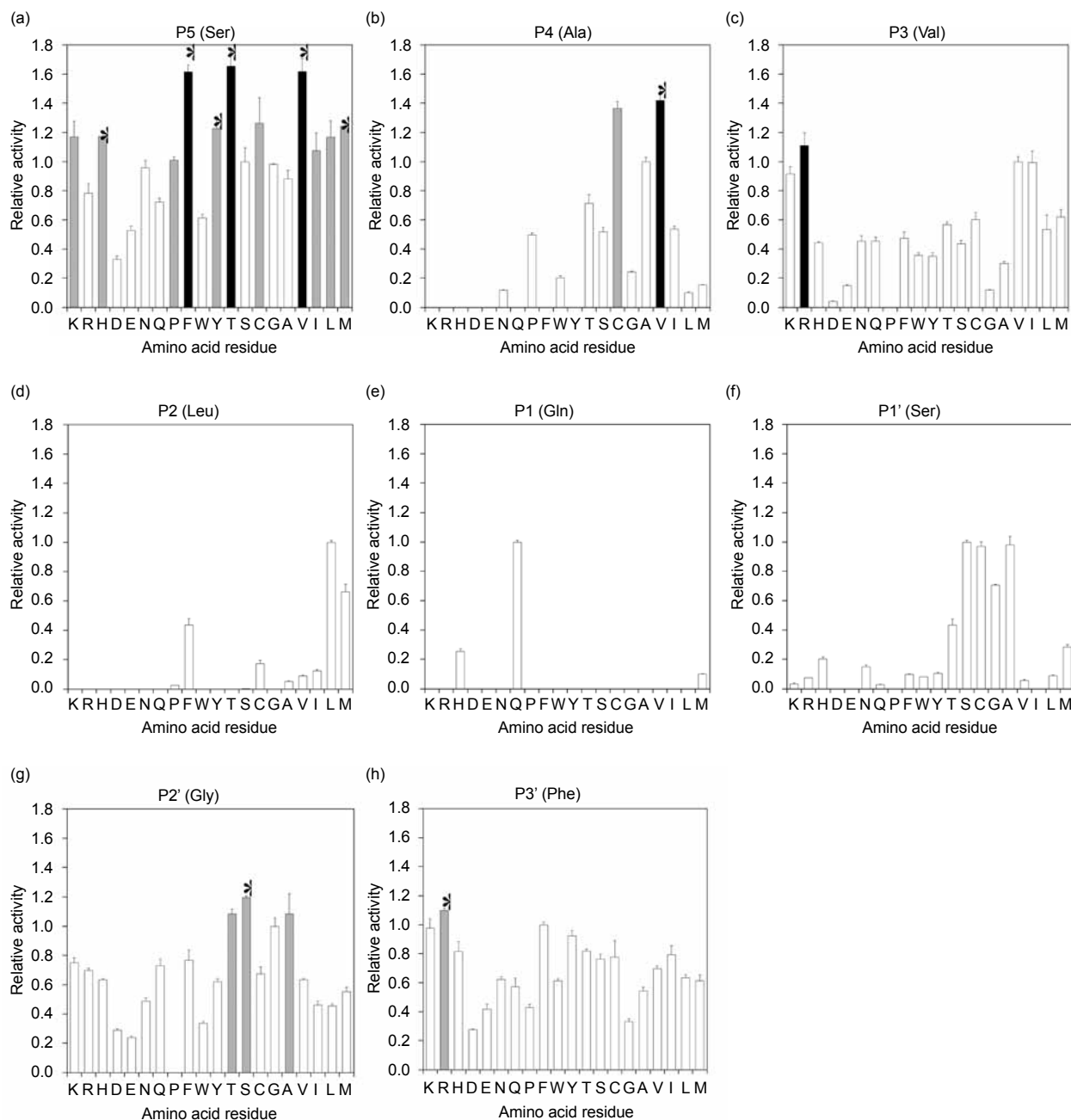
FIG 1. Substrate-specificity profiling of the P5 to P3' positions of SARS-CoV M^pro

Saturation mutagenesis is performed at the P5 to P3' positions of the autocleavage sequence of M^pro to create 19×8 variant substrate sequences. The k_{cat}/K_m values of M^pro on these variant substrate sequences are determined, and their activity relative to the wild-type sequence is shown. Substitutions resulted in higher activities are labelled in grey, whereas those selected for the design of super-active substrate sequence are labelled in black
* Significantly higher relative activity than that of the WT substrate

larger residues were also allowed. Only substitution with Pro resulted in a substrate sequence that could not be cleaved. Substitutions with Thr, Ser, and Ala resulted in a better substrate than the wild-type sequence. At the P3' position, although the substrate preference was loose, positively charged residues (Lys, Arg) were consistently better than negatively charged residues (Glu, Asp).

Substrate-specificity profiling suggested that single substitutions at the P5 to P3 positions affected the relative activities of the substrate sequences. We then combined the best substitutions at these positions to determine whether we could generate an even better substrate sequence.[1] Most of the substitutions could significantly improve relative activity. Among these 'super-reactive' variant,

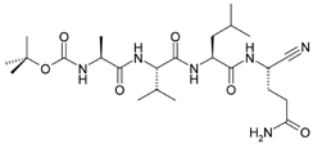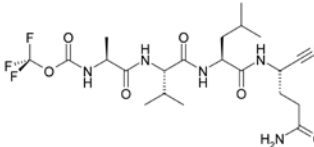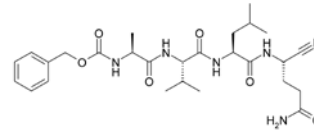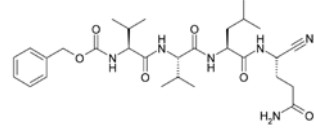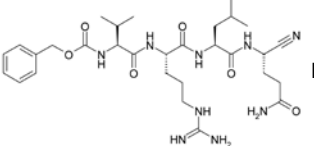'TVRLQ' and 'VVRLQ' were the best with relative activities of >2.5.

The M^pro activity on the 19x8 variant substrate sequences was determined by profiling the substrate specificity at each of the P5 to P3' positions (Fig 1). This systematic profiling study provided a rationale basis for peptidomimetic inhibitor design. Leu and Gln were the best choice for the P2 and P1 positions in the design of a peptidomimetic inhibitor. Residues at the P5 to P3 positions were important in the best substrate for M^pro. The trend observed was further confirmed by creating 'super-reactive' substrate via double and triple substitutions.[1]

The design and synthesis of peptidomimetic inhibitors have been reported.[2] First, we tried two warheads, nitrile and propargylamide groups, and found that only the nitrile group could serve as an efficient warhead. Next, we tested if the N-terminal protective group and the substrate sequence would influence the inhibitory effect (Table).[2] Our data suggested that the best protecting group was Cbz, and the best substrate sequence was AVLQ. Noteworthy, Cbz-VRLQ-CN had no observable inhibition on M^pro (Table). The nitrile warhead was not stable and was hydrolysed to amide (confirmed by mass spectrometry) in the inhibitor Cbz-VRLQ-CN, rendering it ineffective. The best inhibitor synthesised was Cbz-AVLQ-CN, with an M^pro value of 5 μM (Table).[2] To better understand how this inhibitor interacts with the M^pro, we determined the crystal structure of M^pro in complex with the inhibitor Cbz-AVLQ-CN. In the crystal structure, the nitrile warhead of the Cbz-AVLQ-CN inhibitor was attacked by the –SH group of the active site residue Cys145 to form a covalent-linked structure analogous to the acyl-enzyme intermediates (Fig 2). As a result, the side-chains of the inhibitor could form optimal interactions with the M^pro. Our structure of the M^pro-inhibitor complex also explained why Cbz was a better protecting group. The benzene ring of Cbz is inserted in a pocket to form favourable hydrophobic interactions with the Pro168, aliphatic chain of Glu166, and Val at the P3 position of the inhibitor. With the crystal structure of M^pro-inhibitor complex, we are in a much better position to improve the inhibitor activity against M^pro in the future.

Acknowledgements

Table. IC50 values of the peptidomimetic inhibitors synthesised

Inhibitor	Chemical structure	IC50
Boc-AVLQ-CN		52±12 uM
TFA-AVLQ-CN		>64 uM
Cbz-AVLQ-CN		5±1 uM
Cbz-VVLQ-CN		19±6 uM
Cbz-VRLQ-CN		No inhibition
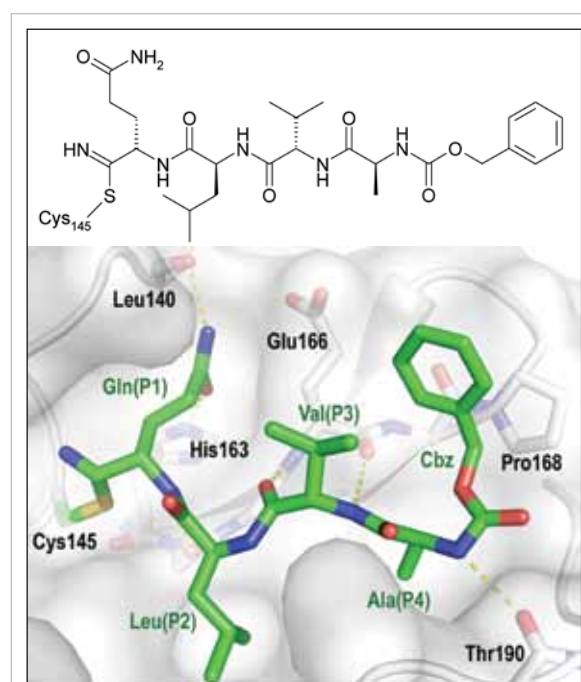
FIG 2. Structure of SARS-CoV Mpro in complex with inhibitor Cbz-AVLQ-CN
The inhibitor is covalently linked to the SG atom of Cys145. Hydrogen bonds are indicated as dotted lines

based broad-spectrum peptidomimetic inhibitors for coronavirus 3C-like proteases. *Eur J Med Chem* 2013;59:1-6.

References

1. Chuck CP, Chong LT, Chen C, Chow HF, Wan DC, Wong KB. Profiling of substrate specificity of SARS-CoV 3CL. PLoS One 2010;5:e13197.
2. Chuck CP, Chen C, Ke Z, Wan DC, Chow HF, Wong KB. Design, synthesis and crystallographic analysis of nitrile-based broad-spectrum peptidomimetic inhibitors for coronavirus 3C-like proteases. Eur J Med Chem 2013;59:1-6.
3. Ziebuhr J, Snijder EJ, Gorbalenya AE. Virus-encoded proteinases and proteolytic processing in the Nidovirales. J Gen Virol 2000;81:853-79.
4. Hegyi A, Ziebuhr J. Conservation of substrate specificities among coronavirus main proteases. J Gen Virol 2002;83:595-9.
5. Ziebuhr J, Heusipp G, Siddell SG. Biosynthesis, purification, and characterization of the human coronavirus 229E 3C-like proteinase. J Virol 1997;71:3992-7.

Profiling of substrate-specificity and rational design of broad-spectrum peptidomimetic inhibitors for main proteases of coronaviruses

CP Chuck, ZH Ke, C Chen, DCC Wan, HF Chow, KB Wong *

KEY MESSAGES

1. Substrate specificities of the main proteases from group 1, 2a, 2b, and 3 coronaviruses were comprehensively profiled at P5 to P3' positions.

2. Despite subtle differences in substrate specificities identified at P1, P2, and P4 positions, the main proteases from different strains of coronaviruses share many similarities, suggesting the feasibility of developing a broad-spectrum inhibitor.

3. `Super-active' substrates with >4-fold increases in activity were created by combining multiple favourable substitutions.

4. Cbz-AVLQ-CN is a broad-spectrum inhibitor effective against six different strains of

coronaviruses (HCoV-NL63, HCoV-OC43, HCoV-HKU1, SARS-CoV, IBV) with IC_{50} values of 1.3 to 4.6 µM.

[1] CP Chuck, [2] ZH Ke, [2] C Chen, [3] DCC Wan, [2] HF Chow, [1] KB Wong *

The Chinese University of Hong Kong:
[1] *School of Life Sciences*
[2] *Department of Chemistry*
[3] *School of Biomedical Sciences*

* Principal applicant and corresponding author: kbwong@cuhk.edu.hk

Introduction

Coronavirus (CoV) infection causes a number of respiratory tract diseases in human.[1] The most infamous was the outbreak of severe acute respiratory syndrome (SARS) in 2003. Coronaviruses can be classified into group 1, 2a, 2b, and 3 based on sequence analysis.[2] Most of the CoVs that infect humans belong to group 1 (eg HCoV-NL63, HCoV-229E), 2a (eg HCoV-OC43, HCoV-HKU1), and 2b (SARS-CoV). Because of the high frequency of mutations and the possibility of animal-to-human transmission, CoVs remain a potential threat to public health. Currently, there is no approved drug to combat CoV infection. The development of broad-spectrum inhibitors that can target all strains of CoV is preferable as first-line defence against CoV infection.

The main protease (M^{pro}) is an attractive target for such broad-spectrum inhibitors. The M^{pro} is responsible for proteolytic processing of polyproteins 1a and 1ab, which release at least 15 non-structural proteins that are essential for viral replication. The M^{pro} is a cysteine protease, which uses an invariant cysteine residue to attack the scissile peptide bond. Although the substrate specificities of SARS-CoV Mpro have been extensively studied,[3] there is no comprehensive study on substrate specificities on M^{pro} from other CoVs. We therefore profiled the substrate specificities of

M^{pro} from group 1 (HCoV-NL63), 2a (HCoV-OC43), 2b (SARS-CoV), and 3 (IBV) using a 19x8 substrate library.[4] Guided by substrate specificities obtained, we created 'super-active' substrates by combining multiple favourable substitutions. Finally, we synthesised peptidomimetic inhibitors based on the nitrile warhead, and demonstrated broad-spectrum inhibition of six different strains of CoVs.

Methods

Profiling of substrate specificity

This study was conducted from January 2010 to December 2011. Cloning, expression, and purification of M^{pro} from HCoV-NL63, HCoV-OC43, SARS-CoV were performed as described.[3] The purification of the19x8 substrate library, and the assay of protease activity of different Mpro against the substrate library were as described.[3]

Synthesis and assay of inhibitors

Peptidomimetic inhibitors were synthesised by coupling a nitrile warhead to the C-terminus of a peptide using the mixed anhydride method, and were protected at the N-terminus by a carboxybenzyl (Cbz) group. The protease activity in the presence of 0.5 to 256 µM of inhibitors was measured using the FRET assay.[3] The IC_{50} values were obtained by fitting the protease activity to a four-parameter logistics curve.

Structure determination of M^pro^-inhibitor complex

SARS-CoV M^{pro} without the inhibitor was crystallised in 50mM-(N-morpholino)ethane-sulfonic acid, pH 5.5, 8.5% (w/v) of polyethylene glycol 6000, 10% (v/v) glycerol, 3% (v/v) DMSO, 1 mM ethylenediaminetetraacetic acid and 1 mM dithiothreitol at 16ºC using the hanging-drop-vapour-diffusion method. Inhibitor (600 µM) was added to 5 ml of mother liquor containing single crystals of SARS-CoV M^{pro}, and was incubated overnight at 16ºC. The crystals were cryoprotected by 20% (v/v) glycerol, and diffraction data were collected in an in-house Rigaku FRE+ X-ray source, and were processed by the CCP4 program suite. The structure of the M^{pro}-inhibitor complex was solved by molecular replacement, built interactively by the program COOT, and refined by the program PHENIX.

Results

Substrate-specificities of M^pro^ from group 1, 2a, 2b, and 3 coronaviruses

The substrate specificities of M^{pro} were profiled from different groups of CoVs using a 19x8 substrate library.[4] All of the M^{pro} could cleave the sequence SAVLQ↓SGF with specific activities of 443±11, 124±13, 180±5, and 174±19 min^{-1} mM^{-1} for HCoV-NL63 (group 1), HCoV-OC43 (group 2a), SARS-CoV (group 2b), and IBV (group 3), respectively (Fig 1).[3]

Engineering of a 'super-active' substrate sequence

Multiple favourable substitutions were combined to determine if a 'super-active' substrate sequence could be engineered. Based on the substrate specificities profiled, all M^{pro} favoured a Val at P5 and a Arg at P3 positions, with relative activities of 1.23 to 1.80 and 0.97 to 1.73, respectively (Table).[3] By combining both substitutions, the activity was increased to 1.70 to 3.24 (Table). The doubly substituted sequence, VARLQ↓SGF, appeared to be a good broad-spectrum substrate for all M^{pro}.

Substitution of P4-Val and P4-Pro resulted in higher than wild-type activity for SARS-CoV and IBV M^{pro}, respectively (Fig 1).[3] Based on this observation, the P4-Val or P4-Pro substitutions were introduced to VARLQ↓SGF, and two triply substituted substrates were generated. The protease activity for the triply substituted substrate (VVRLQ↓SGF) was further increased to 2.5 for SARS-CoV M^{pro} (Table).[3] This increase in activity for SARS-CoV M^{pro} was achieved at the expense of reduced activity for other M^{pro}. Similarly, >4-fold increase for IBV M^{pro} was achieved by combining all favourable substitutions (P3-Arg, P4-Pro, and P5-Val). The triply substituted sequence (VPRLQ↓SGF) represented the best 'super-active' sequence for IBV M^{pro}.

Design, synthesis, and characterisation of broad-spectrum peptidomimetic inhibitors

The autocleavage sequence (SAVLQ↓SGF) could

FIG 1. Substrate specificity of Mpro at P5 to P3' positions. The relative activities of Mpro from HCoV-NL63, HCoV-OC43, SARS-CoV, IBV are represented by circles, squares, diamond, and triangles, respectively. Significantly higher relative activities (P<0.001) are represented by filled symbols. This figure was adapted from: Chuck CP, Chow HF, Wan DC, Wong KB. Profiling of substrate specificities of 3C-like proteases from group 1, 2a, 2b, and 3 coronaviruses. PLoS One 2011;6:e27228
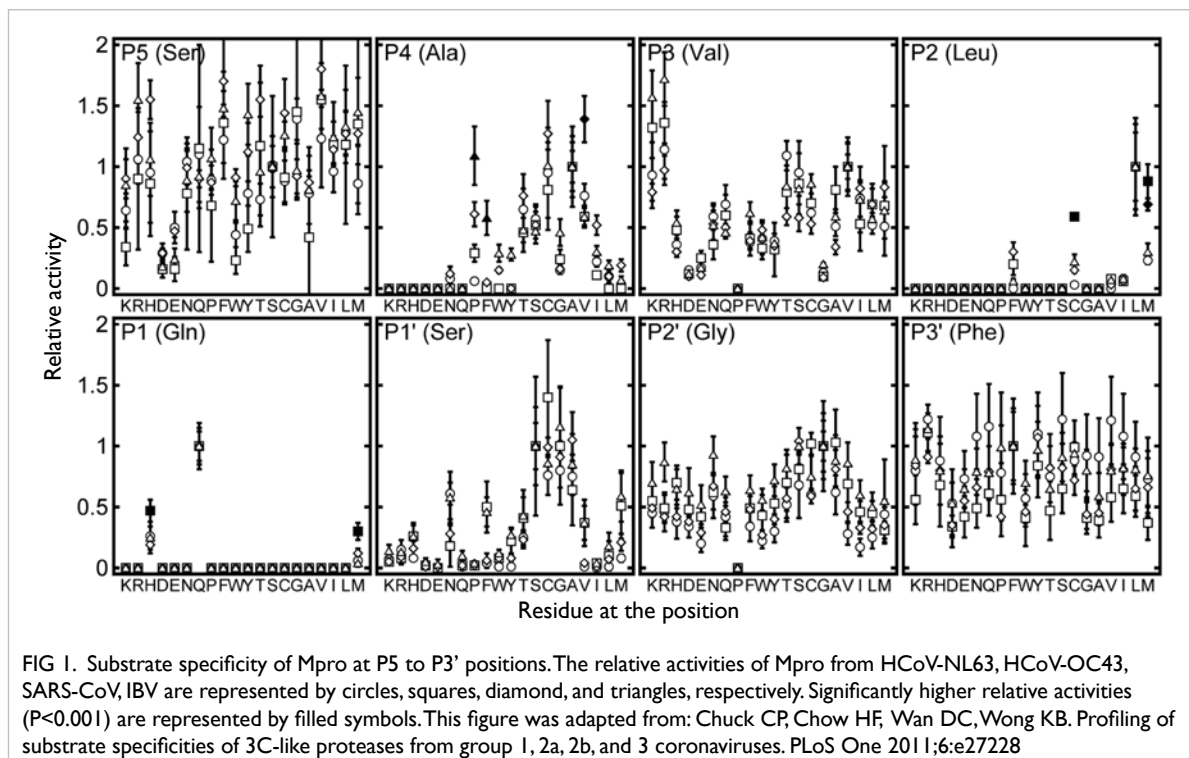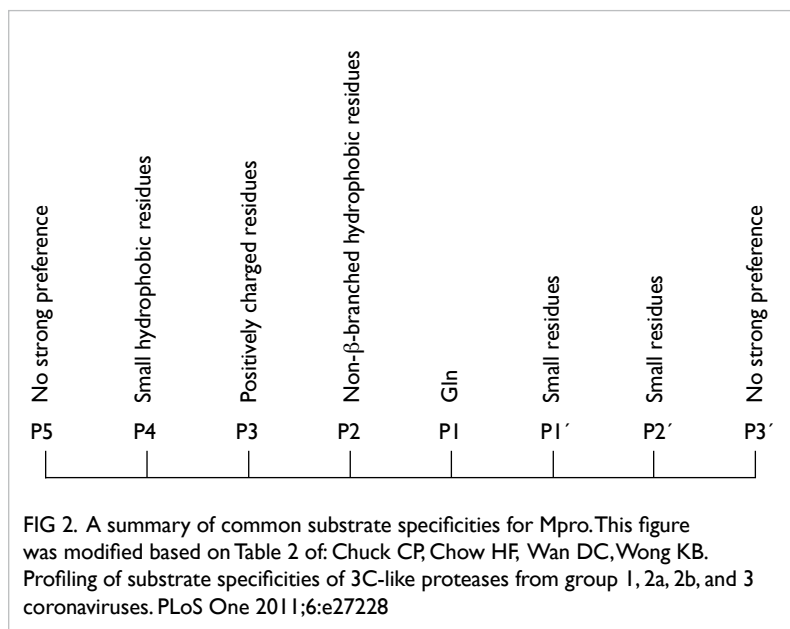
TABLE. Relative protease activity of doubly and triply substituted substrate variants. This table was adapted from: Chuck CP, Chow HF, Wan DC, Wong KB. Profiling of substrate specificities of 3C-like proteases from group 1, 2a, 2b, and 3 coronaviruses. *PLoS* One 2011;6:e27228

Substrate sequence	HCoV-NL63 (group 1)	HCoV-OC43 (group 2a)	SARS-CoV (group 2b)	IBV (group 3)
VAVLQ↓SGF	1.23±0.40	1.55±0.30	1.80±0.31	1.58±0.27
SARLQ↓SGF	1.14±0.24	1.36±0.17	0.97±0.12	1.72±0.22
VARLQ↓SGF	1.70±0.07	1.87±0.17	1.70±0.17	3.24±0.37
SPVLQ↓SGF	0.06±0.01	0.29±0.12	0.61±0.10	1.09±0.24
VPRLQ↓SGF	0.15±0.04	0.91±0.12	0.99±0.12	4.33±0.98
SVVLQ↓SGF	0.76±0.10	0.59±0.07	1.39±0.19	0.59±0.09
VVVLQ↓SGF	1.23±0.06	0.60±0.05	1.97±0.19	0.86±0.05
VVRLQ↓SGF	1.63±0.07	0.55±0.04	2.50±0.51	2.19±0.13

FIG 2. A summary of common substrate specificities for Mpro. This figure was modified based on Table 2 of: Chuck CP, Chow HF, Wan DC, Wong KB. Profiling of substrate specificities of 3C-like proteases from group 1, 2a, 2b, and 3 coronaviruses. PLoS One 2011;6:e27228

be cleaved efficiently by all M^{pro} tested. Based on a tetrapeptide-based inhibitor (Cbz-AVLQ-CN), the nitrile group was an efficient warhead in inhibiting M^{pro} with IC_{50} values of 4.6±0.2 µM.[5] The roles of P5 and P6 residues were then tested by extending the length of the peptide sequence and creating a hexapeptide inhibitor (Cbz-TSAVLQ-CN). Notably, inclusion of P5-Ser and P6-Thr residues did not improve the efficacy, as the IC_{50} value of the hexapeptide inhibitor was 39±1 µM.[5]

To understand the structural basis of the enzyme-inhibition interaction, the crystal structure of Cbz-TSAVLQ-CN in complex with SARS-CoV M^{pro} (PDB code: 3VB6) was compared to the structure of Cbz-AVLQ-CN in complex with SARS-CoV M^{pro} (PDB code: 3VB5).[5] The nitrile warhead of both inhibitors was covalently attached to the thiol group of the active site cysteine residue (Cys145). Residues at the P1 to P4 positions were well defined and fitted nicely into the S1-S4 substrate binding pockets of M^{pro}. In the crystal structure of Cbz-AVLQ-CN in complex with M^{pro}, the benzene group of the Cbz-AVLQ-CN was ordered and located in a pocket formed by Glu166-Pro168. In contrast, in the crystal structure of Cbz-TSAVLQ-CN in complex with M^{pro}, no electron density was observed for the Cbz protective group, P5-Ser, and P6-Thr residues. This suggested that they were disordered, probably due to the lack of a defined interaction with the M^{pro}, which may explain why the hexapeptide inhibitor had a higher IC50 value than the tetrapeptide inhibitor.

For tetrapeptide-based inhibitors, measurement of IC_{50} values of Cbz-AVLQ-CN was extended to other M^{pro}. The IC_{50} values were 2.8±0.1, 2.3±0.1, 1.6±0.1, 1.3±0.1, 4.6±0.2, 3.7±0.2 µM for HCoV-NL63, HCoV-229E, HCoV-OC43, HCoV-HKU1, SARS-CoV, and IBV, respectively.[5] The inhibition of Cbz-AVLQ-CN was specific to M^{pro}, as there was no detectable inhibition at 0.5 to 256 µM against the control cysteine protease (Caspase 3).

Discussion

In this study, we comprehensively profiled the substrate specificity of M^{pro} from HCoV-NL63 (group 1), HCoV-OC43 (group 2a), SARS-CoV (group 2b), and IBV (group 3) using a 19x8 substrate library. Despite subtle differences, all M^{pro} share many similarities in their substrate preferences. The common substrate specificities of M^{pro} are summarised in Figure 2. The substrate preference at different positions was in general additive, as combining several favourable substitutions further increased the protease activities of M^{pro}.

That all M^{pro} shares similarity in their substrate specificities implies that it is feasible to design a broad-spectrum peptidomimetic inhibitor for M^{pro} from various strains of CoVs. The autocleavage sequence (SAVLQ↓SGF) is a very good broad-spectrum substrate, which was cleaved efficiently by all M^{pro} with specific activity ranging from 124 to 443 $min^{-1} mM^{-1}$.[3] This sequence is the starting point for further iteration in the design of broad-spectrum inhibitors for M^{pro}. By comparing the IC_{50} values of Cbz-TSAVLQ-CN and that of Cbz-AVLQ-CN, increasing the length of the peptide from tetrapeptide to hexapeptide did not improve inhibition.[5] This observation was justified because the P5-Ser and P6-Thr residues were disordered in crystal structure of Cbz-TSAVLQ-CN in complex with M^{pro}, as they did not have a significant interaction with the active site of the enzyme.[5] In contrast, the protective carbobenzyloxy group located at the C-terminus of P4 residues helped stabilise the enzyme-inhibitor complex. As P5 and P6 residues did not contribute

to an improved inhibition, the tetrapeptide-based inhibitor (Cbz-AVLQ-CN) was probably a good candidate for broad-spectrum inhibition against M^{pro}. In fact, this inhibitor could efficiently inhibit M^{pro} from six different strain of CoV, with IC_{50} values ranging from 1.3 to 4.6 µM.

Conclusions

We comprehensively profiled the substrate specificities of M^{pro} from group 1, 2a, 2b, and 3 CoVs at P5 to P3' positions. Differences and similarities in substrate specificities were identified. 'Super-active' substrates with >4-fold increase in activity were engineered by combining multiple favourable substitutions. Nitrile-based peptidomimetic inhibitors were effective against M^{pro}. Inclusion of P5 and P6 residues did not improve inhibitor efficacy, but rather, it was the N-terminal Cbz protective group that provided better enzyme-inhibitor interactions. The Cbz-AVLQ-CN inhibitor was a broad-spectrum inhibitor, as it could inhibit M^{pro} from six different strains of CoVs with IC_{50} values of 1.3 to 4.6 µM.

Acknowledgements

References

1. Sloots TP, Whiley DM, Lambert SB, Nissen MD. Emerging respiratory agents: new viruses for old diseases? J Clin Virol 2008;42:233-43.
2. Woo PC, Lau SK, Huang Y, Yuen KY. Coronavirus diversity, phylogeny and interspecies jumping. Exp Biol Med (Maywood) 2009;234:1117-27.
3. Chuck CP, Chow HF, Wan DC, Wong KB. Profiling of substrate specificities of 3C-like proteases from group 1, 2a, 2b, and 3 coronaviruses. PLoS One 2011;6:e27228.
4. Chuck CP, Chong LT, Chen C, Chow HF, Wan DC, Wong KB. Profiling of substrate specificity of SARS-CoV 3CL. PLoS One 2010;5:e13197.
5. Chuck CP, Chen C, Ke Z, Wan DC, Chow HF, Wong KB. Design, synthesis and crystallographic analysis of nitrile-based broad-spectrum peptidomimetic inhibitors for coronavirus 3C-like proteases. Eur J Med Chem 2013;59:1-6.

Behavioural changes in relation to risk perception and prevention of avian and human influenza in Hong Kong, 2006 to 2010

R Fielding *, BJ Cowling, Q Liao, WWT Lam

KEY MESSAGES

1. Declines in buying live poultry have not been matched with declines in touching when buying.

2. Continued buying of live poultry was associated with declines in perceived risk of influenza A/H5N1 infection.

3. Most food preparation and hand hygiene practices were endorsed by >95% of respondents.

4. Population levels of trust in government and media messages about influenza A/H5N1 were unchanged, but there was an apparent increase in the degree of trust in informal sources of information, such as friends and peer opinion, and behaviour in dictating appropriate protective responses against influenza A/H5N1.

R Fielding *, BJ Cowling, Q Liao, WWT Lam

School of Public Health, The University of Hong Kong

* Principal applicant and corresponding author: fielding@hku.hk

Introduction

According to two population surveys of poultry exposure and risk perception in Hong Kong, live poultry exposures among the Hong Kong population through live poultry purchases decreased by >60% (1.1 million person-chicken exposures annually) between 2004 and 2006. This was due to the reduction of imports and, to a lesser extent, reduced touching during purchases, reflecting impacts of public health education messages.[1,2] Periodic isolation of avian influenza viruses from live chickens has prompted changes in policies such as a monthly rest day in local wet markets when all birds are sold or slaughtered and the market is emptied for disinfection (from 2001), an increase to two rest days per month (from 2003), and most recently no live poultry being kept overnight at retail outlets (since June 2008).[3] The plan to stop all direct sales of live poultry in wet markets and introduce central slaughtering for chickens appears to have been shelved.

Although policy can ameliorate environmental risk (defined as the external risk to individuals), risk perception is more important for motivating health behavioural change, which may reduce risks secondary to personal lifestyle choices.[4] Perceived risk may decline as minimising human-chicken contact decreases peoples' perceived need to take preventive action. This may lead to increased population risk (based on the law of unintended consequences) of other influenza and upper respiratory viruses due to reduction in preventive behaviours. Common preventive measures for avian influenza such as personal hygiene, social distancing, and health services utilisation are also important preventive measures for other infectious diseases, including human influenza and other upper respiratory diseases.[5] Therefore, it is important to understand how policies impact on behaviour. We conducted a follow-up survey in 2010 and compared findings to those from our previous studies of avian influenza risk perception and live poultry exposure in 2006.[1]

Methods

This study was conducted from December 2009 to August 2010. Telephone survey of 1613 of the 1760 respondents in the 2006 survey[1] who had agreed to be re-contacted was repeated. Respondents completed a telephone survey of mostly Likert-type categorical questions about perceived risk and worry about influenza A/H5N1, adequacy of government response and practice, effectiveness and need of personal hygiene behaviours, as well as household purchasing of live poultry and touching birds during buying. The prevalence of buying and touching in 2010 was compared with that in 2006, as were perceived risk, worry, and protective hygiene practices. Descriptive and multivariate statistics were used to compare the two datasets.

Outcome measures included: (1) live poultry exposure, which was assessed using a series of questions about personal and household buying of live poultry over the past 3 months, touching during purchase, and frequency of purchase[1]; (2) influenza risk perception, worry, and vaccination behaviour, which was assessed using nine questions,[1] which

were either binary (have you had vaccinations?) or in categorical Likert scales; (3) personal hygiene practices and their perceived effectiveness, which were indicated by their level of protective personal hygiene practice (covering mouth when sneezing; washing hands after sneezing, coughing, touching the nose; using liquid soap to wash hands; use of serving utensils; touching lift buttons with protection) using a 5-point Likert scale (from always to never). Eight more questions were asked about how effective respondents felt these practices were; (4) attitudes and knowledge about avian influenza and trust in media and government information, for which 27 statements were presented and respondents were asked to indicate their agreement using a five-point Liker scale (from strongly agree to strongly disagree)[1]; (5) attitudes towards government interventions to prevent avian influenza and their continuation, for which seven Likert-scaled questions (from strongly agree to strongly disagree) about government action to control avian influenza were asked, as were 11 about the need to continue or maintain these practices now; and (6) demographics of respondents, which were adopted from the 2006 survey[1] and supplemented by questions on the structure and health status of the household members.

Results

Of 1630 respondents agreed to be re-contacted, only 680 (42%) could be traced, of whom 461 agreed to complete the repeat questionnaire. Compared with the 2006 survey, in the 2010 survey, 18-to-34-year-old respondents were more likely to have declining perceived risk of influenza A/H5N1 infection (odds ratio [OR]=2.30, 95% confidence interval

[CI]=1.25-4.24) and less H5N1 worry, (OR=2.01, 95% CI=1.10-3.66). Moreover, more educated respondents (OR=1.90, 95% CI=1.09-3.31) and those who were middle-aged (34-to-54-year-old) had less perceived risk from buying live poultry (OR=2.31, 95% CI=1.33-4.01). About 33%, 11%, and 21% of respondents respectively reported perceiving an increased likelihood of H5N1 infection, H5N1 worry, and perceived buying risk. The remaining respondents reported either unchanged risk (28%, 49%, 46%) or declining risk (38%, 40%, 32%). Household buying of live poultry had declined from 73% to 41%, with households buying on average 11.4 chickens/household/year, compared to 14.4 in 2006, and perceptions of increased risk from buying were associated with not buying live poultry (OR=0.34, 95% CI=0.19-0.60). However, touching during buying remained unchanged at ~5%. The mean exposure to live poultry per household per year decreased 38% from 0.72 in 2006 to 0.57 in 2010 (P=0.011).

The prevalence of most personal hygiene practices remained high, except for covering mouth when sneezing/coughing and hand washing frequency; males were less likely to cover the mouth when sneezing/coughing or to use liquid soap for hand washing. These hygiene declines were associated with declining worry about H5N1 (OR=1.61, 95% CI=1.04-2.47).

More than 90% of respondents agreed recommended preventive practices were somewhat or very necessary, except for wearing face masks in wet markets (32%), avoiding crowded places (43%), and using bleach solution in drains daily (33%). After adjustment for demographic factors, associations between direction of change of perceived risk and

TABLE. Association between direction of risk perception changes and protective hygiene practices

Risk perception change	OR (95% CI) [not necessary vs necessary]		
	Need of wearing face mask when visiting wet markets	Need of avoiding crowded places	Need of using 1:99 bleach solution in sink and drain every day
Perceived likelihood			
Increased	0.95 (0.58-1.55)	1.11 (0.66-1.88)	1.11 (0.66-1.87)
Unchanged	1.00	1.00	1.00
Declined	0.79 (0.49-1.28)	1.00 (0.60-1.66)	1.23 (0.74-2.04)
Perceived worry			
Increased	0.57 (0.29-1.12)	0.45 (0.21-0.98)*	0.40 (0.17-0.91)*
Unchanged	1.00	1.00	1.00
Declined	0.86 (0.57-1.29)	0.70 (0.45-1.08)	1.10 (0.72-1.68)
Perceived buying risk			
Increased	0.41 (0.24-0.71)*	0.55 (0.31-0.98)*	0.78 (0.45-1.34)
Unchanged	1.00	1.00	1.00
Declined	0.93 (0.60-1.44)	0.94 (0.60-1.48)	0.93 (0.59-1.47)

* P<0.05

perceptions of hygiene practices indicated that increases in perceived worry were associated with greater perceived need to avoid crowded places and use of bleach for drains, whereas the perceived risk from buying increased with greater perceived need to wear masks and avoidance of crowded places (Table).

There were no significant differences in perceived degree of trustworthiness of government or media messages about influenza A/H5N1, but there were increases in the trustworthiness of informal sources of information from friends, peers and family (P<0.001, Wilcoxon's test). More respondents reported understanding how influenza A/H5N1 infection was caused and knowing how to protect against avian influenza in 2010 than in 2006 (both P<0.001). There were significant declines in the perceived effectiveness of hygiene practices regarding hand washing before touching the face or food and after going out in 2010 than in 2006 (both P<0.001). After adjusting for age and gender, only a history of seasonal influenza vaccination (OR=6.2, 95% CI=2.89-13.28) and perceived likelihood of becoming ill (OR=2.20, 95% CI=1.03-4.72) predicted intention to have seasonal vaccination.

Discussion

There were continuing declines in exposure of the population to influenza A/H5N1 risk from live poultry. Although fewer households bought live poultry, the rate of touching remained the same (5%), which indicates that the exposure risk remains high among those persisting in buying live poultry who were also more likely to report higher odds of perceived declines in influenza A/H5N1 risk. There was a significant proportion of respondents who perceived declining risks and worry from influenza A/H5N1, and those that did so were more likely to reduce their preventive behaviours, particularly wearing face masks and washing hands. These individuals were more often younger or middle-aged and male. Public trust in government messages remained unchanged, but people put more weight on what their friends and peers think and do about preventing influenza A/H5N1, which was a surprising

finding. In other studies, we hypothesised that high levels of informal information trustworthiness were likely when there was a dearth of formal information or when uncertainty was high.[6,7] The results in the current study argued against such an hypothesis and forced us to rethink the dynamics of information trust in influenzas.

Regrettably, we did not obtain a large enough sample to derive the planned structural equation model and so could not test the fully adjusted models as we had planned. Nonetheless, data of this and earlier studies contributed to the first longitudinal description of a population response to a major epidemic, but results should be interpreted carefully, as the proportion of respondents was small.

Acknowledgement

References

1. Fielding R, Bich TH, Quang LN, et al. Live poultry exposures, Hong Kong and Hanoi, 2006. Emerg Infect Dis 2007;13:1065-7.
2. Liao Q, Lam WW, Jiang CQ, et al. Avian influenza risk perception and live poultry purchase in Guangzhou, China, 2006. Risk Anal 2009;29:416-24.
3. Hong Kong SAR Government. Prevention of avian influenza. 2008. Available from: http://www.info.gov.hk/info/flu/eng/index.htm
4. Lupton D. The imperative of health. public health and the regulated body. London: SAGE; 1995.
5. Jefferson T, Foxlee R, Del Mar C, et al. Physical interventions to interrupt or reduce the spread of respiratory viruses: systematic review. BMJ 2008;336:77-80.
6. Liao Q, Cowling BJ, Lam WW, Fielding R. The influence of social-cognitive factors on personal hygiene practices to protect against influenzas: using modelling to compare avian A/H5N1 and 2009 pandemic A/H1N1 influenzas in Hong Kong. Int J Behav Med 2011;18:93-104.
7. Liao Q, Cowling BJ, Lam WW, Fielding R. Factors affecting intention to receive and self-reported receipt of 2009 pandemic (H1N1) vaccine in Hong Kong: a longitudinal study. PLoS One 2011;6:e17713.

Infection attack rates during the epidemic of swine influenza A by tracking temporal changes in age-specific seroprevalence rates

JT Wu *, BJ Cowling, I Hung, YL Lau, JSM Peiris

KEY MESSAGE

Serial cross-sectional serological data are a valuable addition to future surveillance of pandemic influenza and other emerging infectious diseases.

[1] JT Wu *, [1] BJ Cowling, [2] I Hung, [3] YL Lau, [4] JSM Peiris

University of Hong Kong:
[1] *School of Public Health*
[2] *Department of Medicine*
[3] *Department of Pediatrics*
[4] *Department of Microbiology*

* Principal applicant and corresponding author: joewu @ hku.hk

Introduction

During the epidemic of swine influenza A/H1N1 (pdmH1N1) in Hong Kong in 2009, two large-scale serological surveys were conducted to track temporal changes in population-level seroprevalence of pdmH1N1 antibodies.[1] The serological data from our pdmH1N1 serosurveys were combined with daily hospitalisation data from clinical surveillance from e-flu database (managed by the Hospital Authority) to characterise the transmission dynamics, infection attack rates (IARs), and severity of pdmH1N1 during the first wave.

This study aimed to: (1) obtain weekly estimates of age-specific IARs among hospital outpatients; (2) construct a representative description of the epidemic by combining the above results with serological data from daily samples of blood donations at the Hong Kong Red Cross Blood Transfusion Service between June 2009 and January 2010 for serum antibodies specific to this virus; and (3) estimate the reproductive number of the H1N1 virus over the course of the epidemic and the effectiveness of community-wide interventions (eg school closure, vaccination) in reducing the reproductive number.

Methods

Subjects

Serum specimens were collected from three groups of subjects. The first group comprised 13 328 blood donors aged 16 to 60 years from the four largest blood donation centres (Mongkok, Causeway Bay, Kwun Tong, and Tsuen Wan) of the Hong Kong Red Cross Blood Transfusion Service between 12 June and 31 December 2009. The second group comprised 3613 outpatients aged <16 years and >60 years with suboptimal health conditions from the paediatric and adolescent medicine outpatient clinic and the medicine outpatient clinic at the Queen Mary Hospital between 2 September 2009 and 30 April 2010. The third group comprised 151 children aged 5 to 14 years (between November and December 2008) and 766 children aged 5 to 14 years (between September and December 2009) who participated in an independent cohort study of paediatric seasonal influenza vaccination and household transmission of influenza. All subjects were bled once only.

Epidemiological surveillance data

Age-stratified data on virologically confirmed outpatient consultations, hospitalisations, intensive care unit admissions, and deaths associated with pdmH1N1 from 29 April 2009 to 15 November 2009 were provided by the Hospital Authority (the e-flu database). Since May 2009, patients admitted with acute respiratory illnesses routinely underwent laboratory testing for pdmH1N1 virus by molecular methods.

Laboratory methods

Sera were tested for antibody responses to A/California/4/2009 by viral microneutralisation (MN). Each serum sample was tested for MN titre ≥1:20 and ≥1:40. Seroprevalence at a given MN titre cutoff (1:20 or 1:40) was defined as the proportion of individuals whose titres were at or above that cutoff.

Estimation of age-specific incidence

The e-flu hospitalisation data suggested that incidences between 30 June and 15 November 2009 were generated mostly by local transmission, whereas
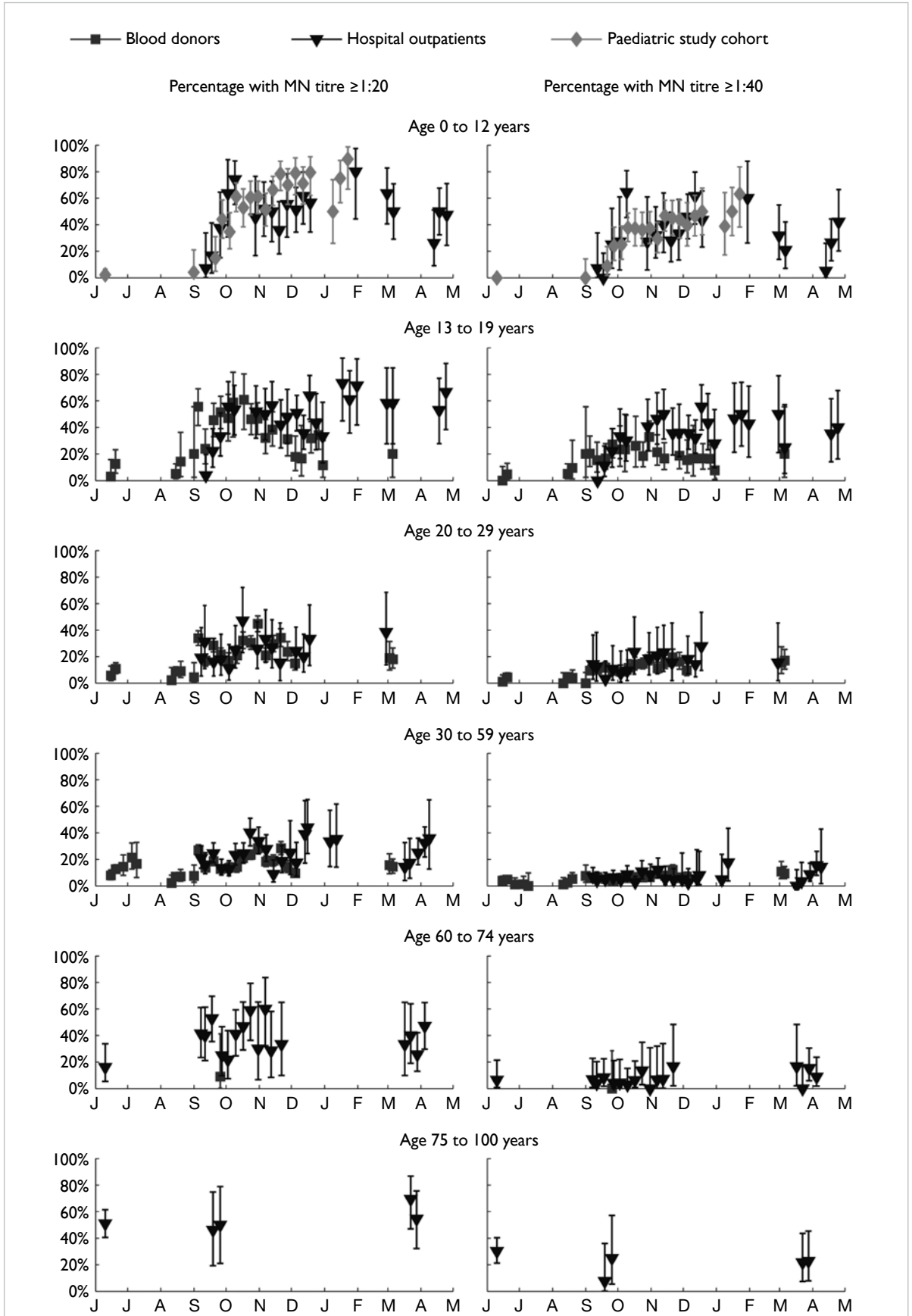
FIG 1. Percentages of age-specific individuals with antibody titres ≥1:20 and ≥1:40 by viral microneutralisation (MN) in Hong Kong between 1 June 2009 and 30 April 2010. Weekly averages and 95% confidence intervals are estimated by the exact binomial method. Data points with a sample size of <10 are not shown. Each tick on the X-axis indicates the first day of month.

incidences from 15 November 2009 onwards were driven mostly by exogenous importation (ie the reproductive number from 15 November onwards was <1). As such, a two-step procedure was used to estimate age-specific incidence from our serological and hospitalisation data: (1) transmission parameters and incidence between 10 June and 15 November 2009 were estimated using an age-structured susceptible-infectious-recovered (SIR) model; and (2) incidences from 15 November 2009 onwards were estimated by dividing daily hospitalisation by the Centre for Health Protection estimated in step 1.

Disease transmission model and statistical inference

An age-structured SIR model with five age-groups (0-12, 13-19, 20-29, 30-59, and ≥60 years) was used to describe the transmission dynamics of pdmH1N1 in Hong Kong between 10 June and 15 November 2009,[2] assuming that those with pre-pandemic MN titre ≥1:20 were immune to pdmH1N1 and that the mean generation time was 2.5 days.[3] Using the age-structured transmission model, seven parameters were estimated by fitting the age-structured SIR

model to our serial cross-sectional serological data and clinical surveillance data: (1) basic reproductive number, (2) susceptibility of each age-group compared to the 20-to-29-year age-group for those who had no immunity, (3) reduction in within-age-group transmission due to school closure, (4) proportion of the age-group that had MN titre at or above the cutoff at the beginning of the pandemic, (5) proportion of infected cases who eventually developed MN titre at or above the cutoff, (6) mean time for MN titre to reach the cutoff after recovery (for those who eventually developed MN titre at or above the cutoff), and (7) case-hospitalisation probability for the age-group. Statistical inference of the parameters was performed using Markov Chain Monte Carlo methods with non-informative priors.

Results

Between 30 June 2009 and 15 November 2009, pdmH1N1 seroprevalence among the three groups of subjects was similar. This implied that IARs were quite similar among blood donors, hospital outpatients, and the vaccination study cohort (Fig 1). As such, the three groups of serological data
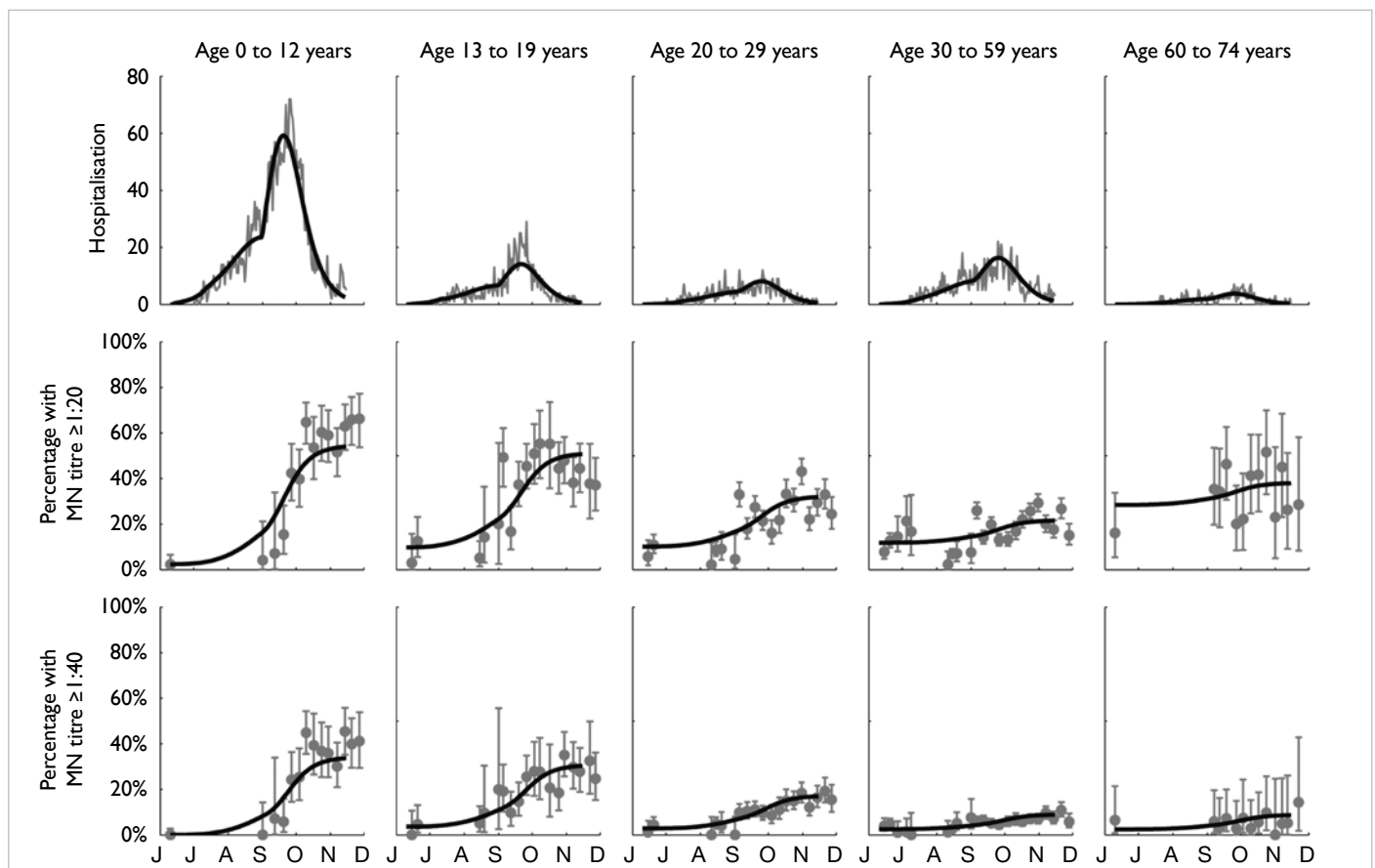

FIG 2. Comparison of the best-fit transmission model with the hospitalisation data and serial cross-sectional serological data: the best-fit hospitalisation and seroprevalence curves are in black colour, whereas the data are in grey colour. Each tick on the X-axis indicates the first day of month.

were aggregated in a transmission modelling analysis, and the estimated IARs thereby were largely applicable to both the general population and hospital outpatients. The best-fit transmission model was reasonably consistent with the serial cross-sectional serological data and hospitalisation data (Fig 2). Regrettably, the proportion of infections that were asymptomatic could not be estimated because most of the subjects did not complete the questionnaire.

Infections were mainly driven by local transmission. The estimated case-hospitalisation probability was 0.23% to 1% for all age-groups. Respectively for the age-groups of 0-12, 13-19, 20-29, 30-59, and 60-74 years, the age-specific IARs were 51% (range, 48-54%), 42% (range, 37-44%), 22% (range, 19-24%), 9.7% (range, 8.5-12.3%), and 10.6% (range, 2.0-17.5%) between 10 June 2009 and 15 November 2009, whereas the estimated age-specific IARs were 13% (range, 12-13%), 5.9% (range, 5.2-6.3%), 6.4% (range, 5.5-7.2%), 4.4% (range, 3.8-5.5%), and 4.7% (range, 0.9-7.7%) between 15 November 2009 and 31 January 2010, assuming that the case-hospitalisation probability was constant over time. The steep drop in IARs with increasing age was consistent with serological studies from other countries.[4,5]

Respectively for the age-groups of 0-12, 13-19, 20-29, 30-59, and 60-74 years, the estimated proportions of individuals who were immune to pdmH1N1 before the endemic were 2.5% (range, 1.0-6.5%), 9.2% (range, 6.4-13.5%), 10% (range, 8.3-12.4%), 11.8% (range, 10.3-12.9%), and 27.2% (range, 21.2-36%), whereas among those who were susceptible to pdmH1N1, the age-groups of 0-12, 13-19, 30-59, and 60-74 years were 2.5 (range, 2.4-2.9), 1.2 (range, 1.1-1.4), 0.5 (range, 0.4-0.6), and 1.4 (range, 0.3-2.1) times more susceptible than the age-group of 20-29 years, respectively.

The estimated basic reproductive number was 1.45 (range, 1.43-1.49), which was consistent with that in earlier studies of pdmH1N1 transmissibility in other populations.[3,6,7] The reproductive number dropped to <1 after mid-September (Fig 3). Among those infected with pdmH1N1, it was estimated that 100% (range, 96-100%) developed MN titre ≥1:20 with a mean delay of 0.4 (range, 0.04-3.7) days after recovery, whereas 64% (range, 53-71%) developed MN titre ≥1:40 with a mean delay of 4.1 (range, 0.5-11.7) days after recovery.

In the best-fit transmission model, compared to the school period during September to December 2009, school closures reduced within-age-group transmission by 52% (range, 36-56%) among the age-
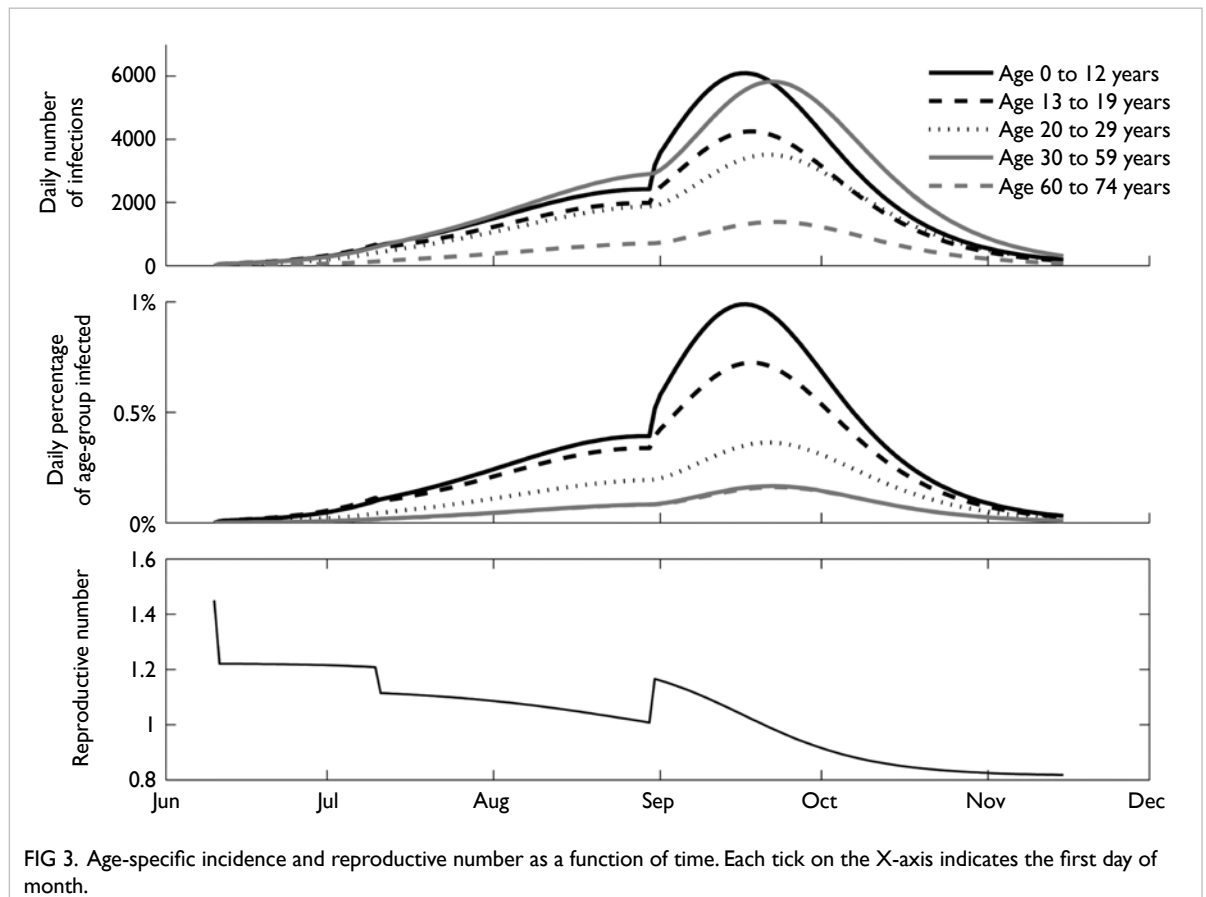

FIG 3. Age-specific incidence and reproductive number as a function of time. Each tick on the X-axis indicates the first day of month.

group of 0-12 years and 26% (range, 18-33%) among the age-group of 13-19 years. Closure of high schools had smaller impact on reducing disease transmission possibly because these teenagers would continue to mix with their peers in other social settings during school closures.

Discussion

It is important to include serological surveys as a component of endemic surveillance. The geographically compact and homogeneously mixed population in the urban environment of Hong Kong enables some degree of confidence in the validity of the estimates of IAR, severity, and transmissibility. The detailed pdmH1N1-reporting system, the wide coverage of the public health care system (that includes >90% of all local inpatient days[8]), and the resource investments since SARS have led to routine laboratory testing for all patients hospitalised with fever or pneumonia. This enables identification of most pdmH1N1 infection–associated hospitalisations. Vaccination did not begin until late December 2009 and therefore had no influence on our estimate of transmissibility, severity, and IAR during the main first wave.

Real-time serial cross-sectional serological data enable accurate estimates of infection attack rates (and from them severity measures) while the endemic is in its nascent stage. These estimates may help public health policymakers to respond to an influenza pandemic, eg assessing the burden that the pandemic would pose on the health care system, and assessing population-level immunity to inform vaccination decisions.

Conclusion

Serial cross-sectional serological data together with hospitalisation data enable accurate estimates of infection attack rate and severity. Serological monitoring should be a key part of updated plans for influenza pandemic preparedness and response.

Acknowledgements

References

1. Wu JT, Ma ES, Lee CK, et al. The infection attack rate and severity of 2009 pandemic H1N1 influenza in Hong Kong. Clin Infect Dis 2010;51:1184-91.
2. Wu JT, Cowling BJ, Lau EH, et al. School closure and mitigation of pandemic (H1N1) 2009, Hong Kong. Emerg Infect Dis 2010;16:538-41.
3. White LF, Wallinga J, Finelli L, et al. Estimation of the reproductive number and the serial interval in early phase of the 2009 influenza A/H1N1 pandemic in the USA. Influenza Other Respir Viruses 2009;3:267-76.
4. Chen MI, Lee VJ, Lim WY, et al. 2009 influenza A(H1N1) seroconversion rates and risk factors among distinct adult cohorts in Singapore. JAMA 2010;303:1383-91.
5. Miller E, Hoschler K, Hardelid P, Stanford E, Andrews N, Zambon M. Incidence of 2009 pandemic influenza A H1N1 infection in England: a cross-sectional serological study. Lancet 2010;375:1100-8.
6. Fraser C, Donnelly CA, Cauchemez S, et al. Pandemic potential of a strain of influenza A (H1N1): early findings. Science 2009;324:1557-61.
7. Yang Y, Sugimoto JD, Halloran ME, et al. The transmissibility and control of pandemic influenza A (H1N1) virus. Science 2009;326:729-33.
8. Leung GM, Wong IO, Chan WS, Choi S, Lo SV; Health Care Financing Study Group. The ecology of health care in Hong Kong. Soc Sci Med 2005;61:577-90.

Effect of *Scutellariae radix (Huangqin)* on preventing rhinovirus-provoked asthmatic inflammation in cultured human bronchial epithelia

WH Ko *, Y Huang

K E Y   M E S S A G E S

1. Infection of human bronchial epithelial cells with rhinovirus has minimal effect on the electrophysiological properties and ion transport processes of these epithelia.

2. The *Scutellariae radix* extract and its major flavonoids could not suppress rhinovirus replication but could promote the secretion of at least two pro-inflammatory cytokines (IL-6 and IL-8) in human bronchial epithelia.

WH Ko *, Y Huang

School of Biomedical Sciences, The Chinese University of Hong Kong

* Principal applicant and corresponding author: whko@cuhk.edu.hk

Introduction

Scutellariae radix (SR), also known as *Huangqin*, is the dried root of *Scutellaria baicalensis Georgi* (Lamiaceae). It is listed in the Chinese Pharmacopoeia and is one of the most widely used Chinese herbal medicines against bacterial infection of the respiratory and the gastrointestinal tracts. The main components of SR (and of all *Scutellaria* species) are baicalein, baicalin, and wogonin. Rhinovirus (RV) infection is the major cause of common colds and the most frequent trigger (up to 85%) for asthma exacerbation.[1] The cellular mechanism by which viral respiratory infections may induce asthma is complex. The bronchial epithelium is the primary target for respiratory viral infections. The viruses must pass through the epithelial barrier to enter the body. At the same time, the viruses infect and replicate in the bronchial epithelial cells. Such infection is associated with airway inflammation, which is partly due to the major basic protein (MBP), a product of the eosinophils. The MBP is increased in upper respiratory viral infections associated with asthma exacerbations,[2] causing virus-induced cellular damage.

The airway surface epithelium itself is responsible for the synthesis and release of cytokines that cause the selective recruitment, retention, and accumulation of various inflammatory cells.[3] Certain inflammatory cytokines alter the fluid and electrolyte transport of the airway epithelium. Therefore, asthma can be considered a disease of the bronchial epithelium, which could contribute to the pathophysiology of airway inflammation. Damage of the surface airway epithelium in asthmatic inflammation is due to the secretion of eosinophil-derived, highly toxic cationic proteins, such as MBP. To simply mimic the damage seen in asthma inflammation, the bronchial epithelium can be challenged with highly charged cationic proteins, such as poly-L-arginine. This study aimed to examine the antiviral activity and therapeutic potential of SR and its three major flavonoids (baicalein, baicalin, and wogonin) in the RV39-infected human bronchial epithelial cell lines (16HBE14o-). In addition, the SR effect on cellular immune responses to experimental RV39 challenge in cells treated with poly-L-arginine, a surrogate of MBP was investigated.

Methods

This study was conducted from December 2010 to November 2011. Cultured human bronchial epithelial cell lines (16HBE14o-) were infected with RV39. Some of the epithelial cells were treated with poly-L-arginine as a surrogate of MBP. Detection and quantification of RV39 RNA in the epithelial cells were performed by quantitative reverse transcription polymerase chain reaction. Cytokine release was quantified by a cytokine antibody array or enzyme-linked immunosorbent assay. The effect of the SR extract and its major flavonoids (baicalein, baicalin, and wogonin) on RV39 mRNA expression in infected 16HBE14o- epithelia was measured by quantitative real-time polymerase chain reaction.

Results

At 72 hours post-infection, RV39 mRNA was detected in 16HBE14o- cells at a multiplicity of

infection (MOI) of 1 (Fig 1). In the presence of the SR extract (10 mg/mL), baicalein (10 mM), or wogonin (10 mM), RV39 mRNA expression increased significantly (P<0.05, n=4-6), compared with control. These doses were selected because at these concentrations the SR extract or its major flavonoids
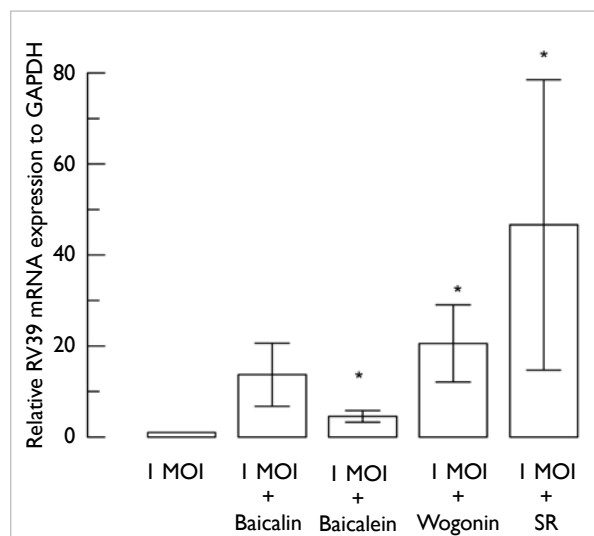

FIG 1. Analysis of rhinovirus (RV39) mRNA expression using quantitative real-time polymerase chain reaction: the epithelia are infected with RV39 at a multiplicity of infection (MOI) of 1 with or without baicalin, baicalein, wogonin, or *Scutellariae radix* (SR) extract. The mean±SE relative expression of RV39 mRNA is normalised to GAPDH and is shown as fold-changes relative to the untreated controls
* P<0.05 compared with a MOI of 1

would not stimulate any increase in short-circuit current (ie chloride ion secretion) in epithelial cells (unpublished data).

Our previous study demonstrated that the inflamed bronchial epithelia mainly secreted two pro-inflammatory cytokines (IL-6 and IL-8) into the supernatant.[4] To measure the secretion of IL-6 and IL-8 more quantitatively, the supernatant samples obtained from normal (non-infected) 16HBE14o- cells stimulated by the SR extract (10 mg/mL), baicalein, baicalin or wogonin (10 mM each) for 72 hours were analysed by ELISA. Exposure to the three major flavonoids significantly increased the release of IL-6 and IL-8, compared to the time-matched control (P<0.05, n=3-12, Fig 2). The SR extract significantly increased the release of IL-8 only (P<0.05, n=3-16).

Whether the SR extract and its major flavonoids had any effect on IL-6 and IL-8 release when the cells were exposed to a low concentration of poly-L-arginine (0.3 mM) and RV39 (MOI of 0.1) was determined. Poly-L-arginine and RV39 did not cause any significant increase in IL-6 and IL-8 levels (P>0.05, n=7-16, Fig 3). In addition, RV39 and poly-L-arginine did not have any additive effect on promoting IL-6 and IL-8 release (data not shown), compared with data obtained from RV39- or poly-L-arginine–treated epithelia. There was a large variability in the release of IL-6 and IL-8. In general, the SR extract or its flavonoids did not show any significant difference in the IL-6 and IL-8 release, compared with cells treated with a combination of poly-L-arginine and RV39 (P>0.05, n=3-16), except for the effect of baicalin or wogonin on IL-6 release.
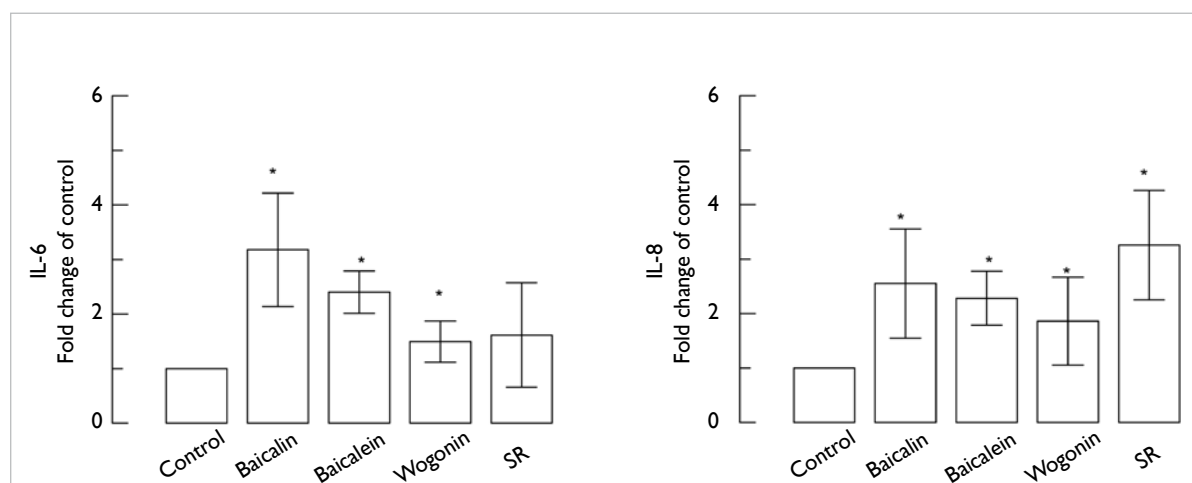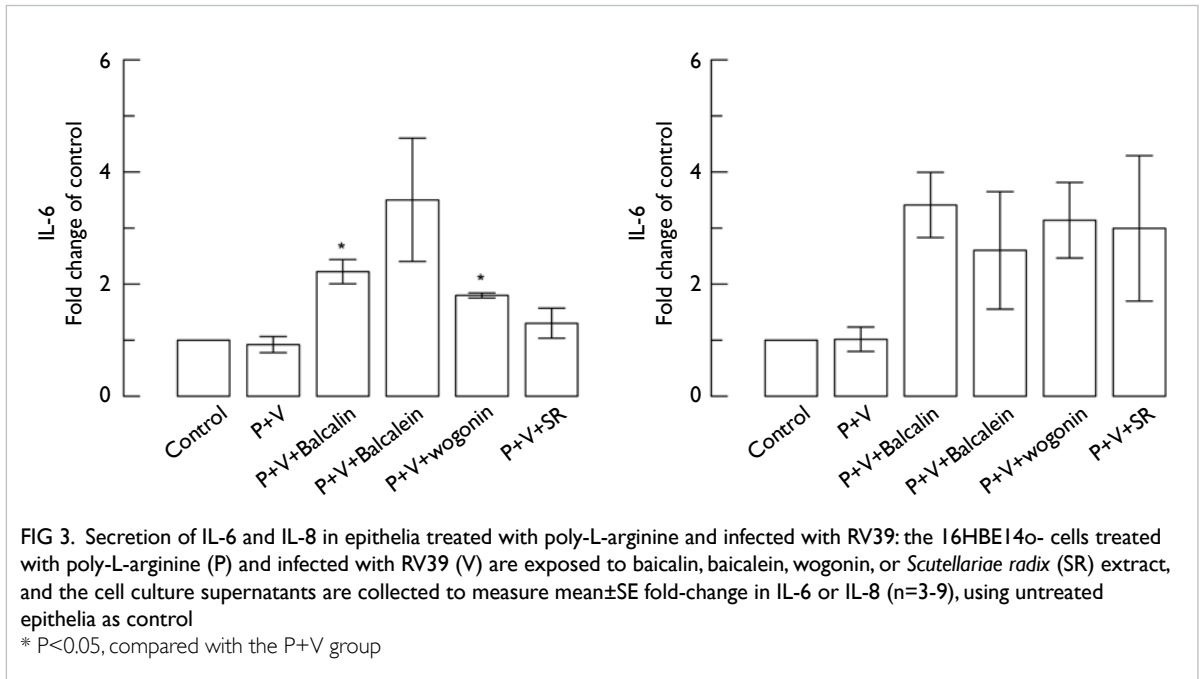

FIG 2. Secretion of IL-6 and IL-8: the 16HBE14o- cells are exposed to baicalin, baicalein, wogonin, or *Scutellariae radix* (SR) extract, and the cell culture supernatants are collected to measure mean±SE fold-change in IL-6 or IL-8 (n=3-9), using untreated epithelia as a control
* P<0.05, compared with control

FIG 3. Secretion of IL-6 and IL-8 in epithelia treated with poly-L-arginine and infected with RV39: the 16HBE14o- cells treated with poly-L-arginine (P) and infected with RV39 (V) are exposed to baicalin, baicalein, wogonin, or *Scutellariae radix* (SR) extract, and the cell culture supernatants are collected to measure mean±SE fold-change in IL-6 or IL-8 (n=3-9), using untreated epithelia as control
* P<0.05, compared with the P+V group

Discussion

Huangqin has been shown to possess anti-inflammatory, antipyretic, anti-allergic, anticonvulsant, antiviral, and antitumour properties.[5] It has been used to treat inflammation-related disorders such as gastroenteritis in China and Japan. Many biological activities of SR are related to its flavonoids (eg baicalein, baicalin, and wogonin).[5] However, our results suggested that the SR extract and its major flavonoids showed no significant inhibition of RV39 replication (antiviral effect), but the relative RV39 mRNA expression was increased. The underlying molecular mechanism of these findings remains unknown. Future experiments should be carried out to measure the virus release to determine whether the enhanced viral mRNA expression is a result of increased replication or altered kinetics of virus release. Although the SR extract and its flavonoids are anti-inflammatory in nature,[5] our cytokine release data showed that they stimulated significant IL-6 and IL-8 release from the 16HBE14o- epithelial cells. To mimic the damage seen in asthma inflammation, the bronchial epithelium was challenged with highly charged cationic polypeptides such as poly-L-arginine, which is similar in structure and function to the biologically active moiety of MBP. At a low concentration of poly-L-arginine, RV39 infection did not promote any increase in IL-6 and IL-8. However, when the epithelia were infected with RV39 in the presence of poly-L-arginine, two flavonoids (baicalin and wogonin) promoted the release of IL-6. This may be due to increased RV39 mRNA expression. Further

experiments are needed to quantify the infectivity of RV39 in 16HBE14o- cells treated with SR extract and its major flavonoids. We cannot exclude the possibility that this is a species- and tissue-specific effect. Nonetheless, our data challenged the traditional belief that the SR extract and it major flavonoids are anti-inflammatory, and also question their therapeutic use as antiviral (anti-rhinovirus) agents, because these agents may affect airway inflammation in asthma.

Acknowledgement

References

1. Nicholson KG, Kent J, Ireland DC. Respiratory viruses and exacerbations of asthma in adults. BMJ 1993;307:982-6.
2. Teran LM, Seminario MC, Shute JK, et al. RANTES, macrophage-inhibitory protein 1alpha, and the eosinophil product major basic protein are released into upper respiratory secretions during virus-induced asthma exacerbations in children. J Infect Dis 1999;179:677-81.
3. Jeffery PK. Pathological spectrum of airway inflammation. In: Page CF, Banner KH, Spina D, editors. Cellular mechanisms in airways inflammation. Basel, Boston, Berlin: Birkhauser Verlag; 2000:1-52.
4. Chow AW, Liang JF, Wong JS, Fu Y, Tang NL, Ko WH. Polarized secretion of interleukin (IL)-6 and IL-8 by human airway epithelia 16HBE14o- cells in response to cationic polypeptide challenge. PLoS One 2010;5:e12091.
5. Li C, Lin G, Zuo Z. Pharmacological effects and pharmacokinetics properties of Radix Scutellariae and its bioactive flavones. Biopharm Drug Dispos 2011;32:427-45.

Antiviral activity of Chinese medicine–derived phytochemicals against avian influenza A (H5N1) virus

VEC Ooi *, PKS Chan, LCM Chiu, SSM Sun , HNC Wong

KEY MESSAGES

1. A screening platform was established to investigate antiviral agents from extracted herbal ingredients against infectious viruses, including avian influenza A (H5N1) virus.

2. More than 30 antiviral herbal fractions and compounds were screened for antiviral activity against H5N1 virus. Three proteins isolated from *Pandanus amaryllifolius* (PYM2), *Narcissus tazett*, and *Polygonatum odoratum* (POL) were identified to have most prominent anti-H5N1 potency. The efficacy of these proteins as antiviral products was investigated, as was molecular cloning and transgenic expression of both PYM2 and POL in bacteria (*Escherichia coli*) and POL in rice plants.

3. The proteins isolated from POL and the soluble seed protein from Gt1/SPPOL/POL transgenic rice showed a significant effect on inhibiting virus infection. This study provides the scientific basis for the use of anti-H5N1 ingredients as chicken feed.

[1] VEC Ooi *, [1] LCM Chiu, [1] SSM Sun, [2] PKS Chan, [3] HNC Wong

The Chinese University of Hong Kong:
[1] Department of Biology
[2] Department of Microbiology
[3] Department of Chemistryg

* Principal applicant and corresponding author: ooi.vincentec@gmail.com

Introduction

In 1997, a highly pathogenic avian influenza A virus (H5N1) in Hong Kong caused death in 6 of 18 infected persons.[1] Subsequent outbreaks of H5N1 avian influenza in several other countries indicated that the virus may be more widely established among the bird population and the environment than previously thought. Human deaths from avian influenza infections have been reported in Indonesia, Vietnam, Thailand, and China. Fortunately, there was no evidence of large-scale human-to-human transmission of the virus. To date only two classes of anti-influenza drugs (amantadine and its derivatives and neuraminidase inhibitors) have been clinically used, but their use may result in the emergence of resistant variants.[2] Phytochemicals such as phenolic compounds, flavonoids[3,4] and proteins such as cyanovirin-N[5] from natural sources may have significant inhibitory effects on influenza A viruses. Our laboratory has isolated, purified, experimentally tested, and identified more than 30 potent antiviral herbal extracts and active compounds that significantly inhibit various human viruses. Three proteins isolated from *Pandanus amaryllifolius* (PYM2), *Narcissus tazett* (NTL), and *Polygonatum odoratum* (POL) were identified to have most prominent anti-H5N1 potency. Their antiviral efficacy and potential as a product was investigated.

Methods

This study was conducted from September 2006 to August 2008. Antiviral activity against influenza A (H1N1) and/or (H3N2) viruses was evaluated in a P2 (Biosafety Level 2) laboratory, whereas that against avian influenza A (H5N1) virus was evaluated in a P3 (Biosafety Level 3) laboratory. A platform for screening antiviral activity against influenza viruses was set up to assess more than 30 experimentally proven antiviral chromatographic fractions and components from Chinese medicinal herbs (Table). The virus yield reduction assay was adopted. Antiviral activity was estimated. Triplicate cultures of Madin-Darby canine kidney cells in 60 mm plastic dishes infected with 100 plaque forming units/0.2 mL of H1N1 or H5N1 virus were set up. The infected cells were fixed and stained, and the virus titre was determined by a cytopathic effect reduction assay and/or plaque assay, which enabled identification of potent anti-H5N1 agents. Molecular characterisation and cloning of the potent antiviral proteins and their transgenic expression in bacteria as the bioreactor was then performed, and the immune modulatory potency of the active antiviral proteins was evaluated. Induction of production and gene expression of the immunomodulatory cytokines by the active antiviral proteins from herbs

was examined in mouse macrophages using specific cytokine primers, total RNA isolated from induced macrophages, and reverse transcription-polymerase chain reaction (RT-PCR). Their effects on the serum level of specific cytokines in mice were evaluated using the enzyme-linked immunosorbent assay (ELISA) 48 hours after an intraperitoneal injection of 5 mg/kg of the proteins.

Results

Of the 30 antiviral chromatographic fractions and components from Chinese medicinal herbs, 10 purified herbal compounds exhibiting potent inhibitory effects against H5N1 virus were identified. Among these, three proteins isolated from PYM2, NTL, and POL had the most prominent anti-H5N1 activity. The results of plaque reduction assays indicated that the proteins significantly inhibited the infectivity of H1N1, H3N2, H5N1, and influenza B viruses. For example, the antiviral effect of PYM2 was dose-dependent, with IC_{50} values of 3.75 µg/mL for H1N1, 0.13 µg/mL for H3N2, 26.03 µg/mL for H5N1, and 0.03 µg/mL for influenza B (Fig 1).

The anti-H5N1 efficacy of these proteins was further investigated for potential product development, possibly as antiviral chicken feed. Molecular cloning and transgenic expression

TABLE. Anti-H5N1 activity of purified phytochemicals and proteins that have been isolated and experimentally proven to have antiviral potential against other viruses*

Purified phytochemicals	Medicinal herbs	Anti–herpes simplex virus	Anti–respiratory syncytial virus	Anti–H5N1 virus
Amentoflavone	Selaginella sinensis		√	+
Wogonin	Scutellaria baicalensis		√	+
Anagyrine	Sophora flavescens		√	ND
Secoiridoid glucoside	Ligustrum lucidum	√	√	ND
Luteollin-7-O-glucoside	Youngia japonica		√	ND
Genkwanol B	Wikstroemia indica		√	ND
Orientin	Trollius chinensis		√	ND
7-O-galloyltricentifavan	Pithecellobium clypearia		√	+
7,4-di-O-galloyltricentifavan	Pithecellobium clypearia		√	+
Daphnoretin	Wikstroemia indica		√	+
Cassanefuranoditerpenoid	Caesalpinia minax	#	√	+
Friedelane triterpenoid	Caesalpinia minax	#	√	+
Lupane-type triterpenoid	Schefflera heptaphylla		√	+
Sesquiterpene	Schefflera heptaphylla		√	+
3,4-di-O-caffeoylquinic acid	Schefflera heptaphylla	√	√	++
3-O-caffeoylquinic acid	Youngia japonica		√	+
Cinnamaldehyde	Cinnamomum cassia	√		+
Lignin-CHO complex	Prunella vulgaris	√		++
Beta-glucan	Pleurotus tuber-regium	√		+
Polysaccharide	Ganoderma lucidum	√		+
Sulfated polysaccharide	Sargassum patens	√		++
Sulfated polysaccharide	Hydroclathrus clathratus	#		++
Polysaccharide	Ardisia chinensis		#	+
Lectin	Pandanus amaryllifolius	√	√	+++
Lectin	Narcissus tazetta	√	√	+++
Lectin	Allium tuberosum	√		++
Lectin	Smilax glabra	√	√	++
Lectin	Dendrobium nobile	√		++
Lipid-transfer protein	Narcissus tazetta	#	√	+
Lectin	Polygonatum odoratum	√	√	+++

* √ denotes having antiviral activity, # having potent activity against other viruses, + weak activity, ++ moderate activity, +++ prominent activity, and ND no detectable activity
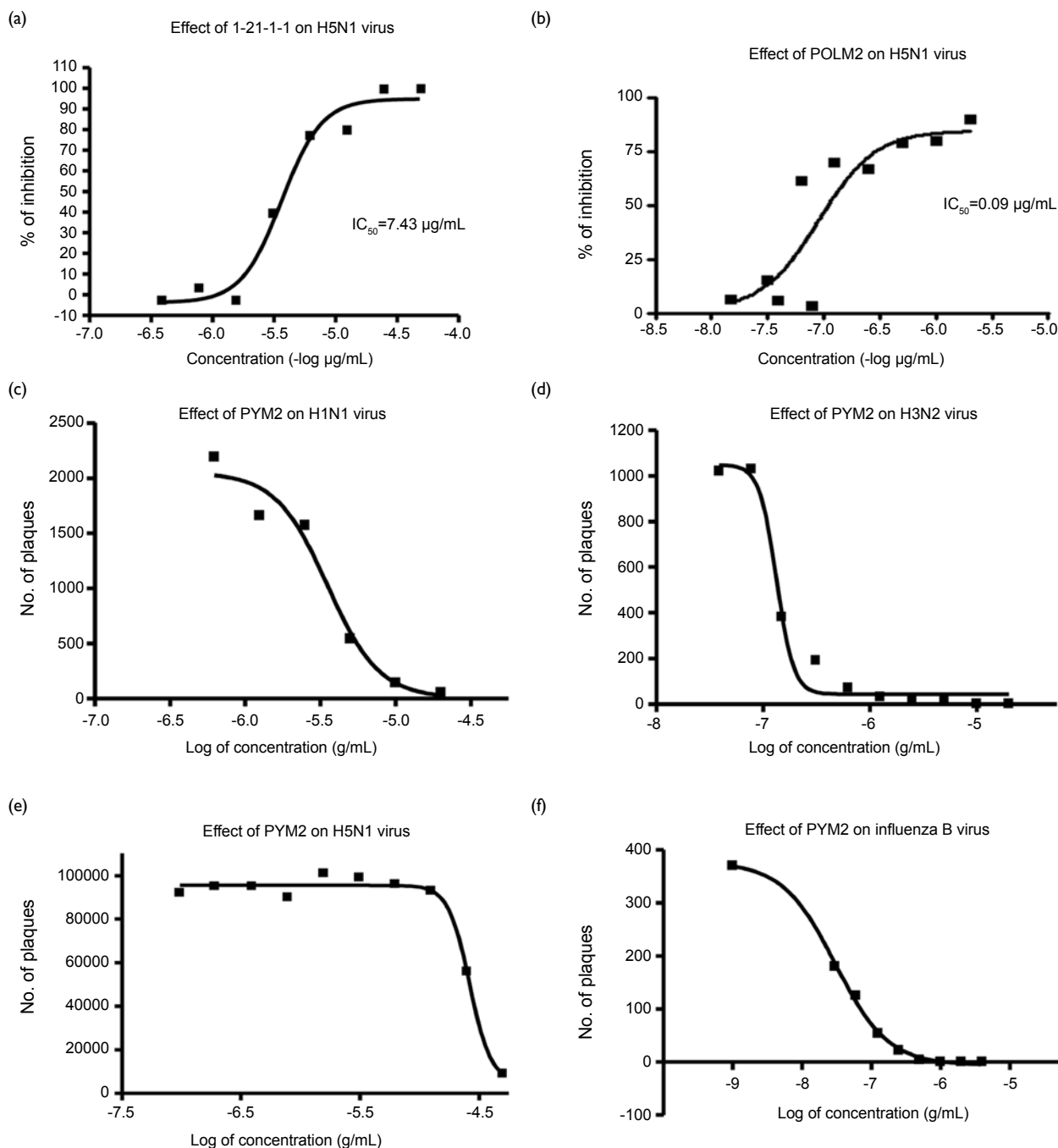
FIG 1. Inhibitory effects of (a) soluble *Polygonatum odoratum* (POL) protein from transgenic rice seed (0.39-100 µg/mL) and (b) purified POL from rhizome of POL (0.010-10 µg/mL) against H5N1 virus, and *Pandanus amaryllifolius* (PYM2) [0.001-50 µg/mL] against (c) H1N1, (d) H3N2, (e) H5N1, and (f) influenza B viruses. Results are based on an extracellular virus yield reduction assay and triplicate cultures of Madin-Darby canine kidney cells

of PYM2 and POL in bacteria (*Escherichia coli*) was investigated for potential application of the expressed proteins against H5N1 virus. For comparison, the rice-derived POL-containing soluble protein (obtained from another project) was confirmed to possess significant potency in terms of inhibiting H1N1 virus with an IC_{50} of 125.5 µg/mL, and H5N1 virus with an IC_{50} of 74.4 µg/mL, whereas POL isolated and purified directly from the leaves of POL exhibited anti-H5N1 activity with an IC_{50} of 6.23 µg/mL (Fig 1). In contrast, the soluble protein from wild type rice sample had no viral inhibitory effect on the three viruses tested, even though up to 1000 µg/mL soluble protein was applied on the viral culture. This suggested that the wild type rice seeds did not contain proteins that could inhibit the viral infections or that its antiviral activities were too low to be measured by this assay (Fig 1).

(a)

(b)

Cytokines	PYM2	POL
IL-1β	↑	↑
IL-1α	↓	↓
IL-2	ND	ND
IL-4	ND	ND
IL-10	+	+
IFN-γ	↑	↑
IL-12p35	↑	↑
TNF-α	↑markedly	↑slightly
TGF-β	↑slightly	+
M-CSF	↓	↑
SCF	↓	+
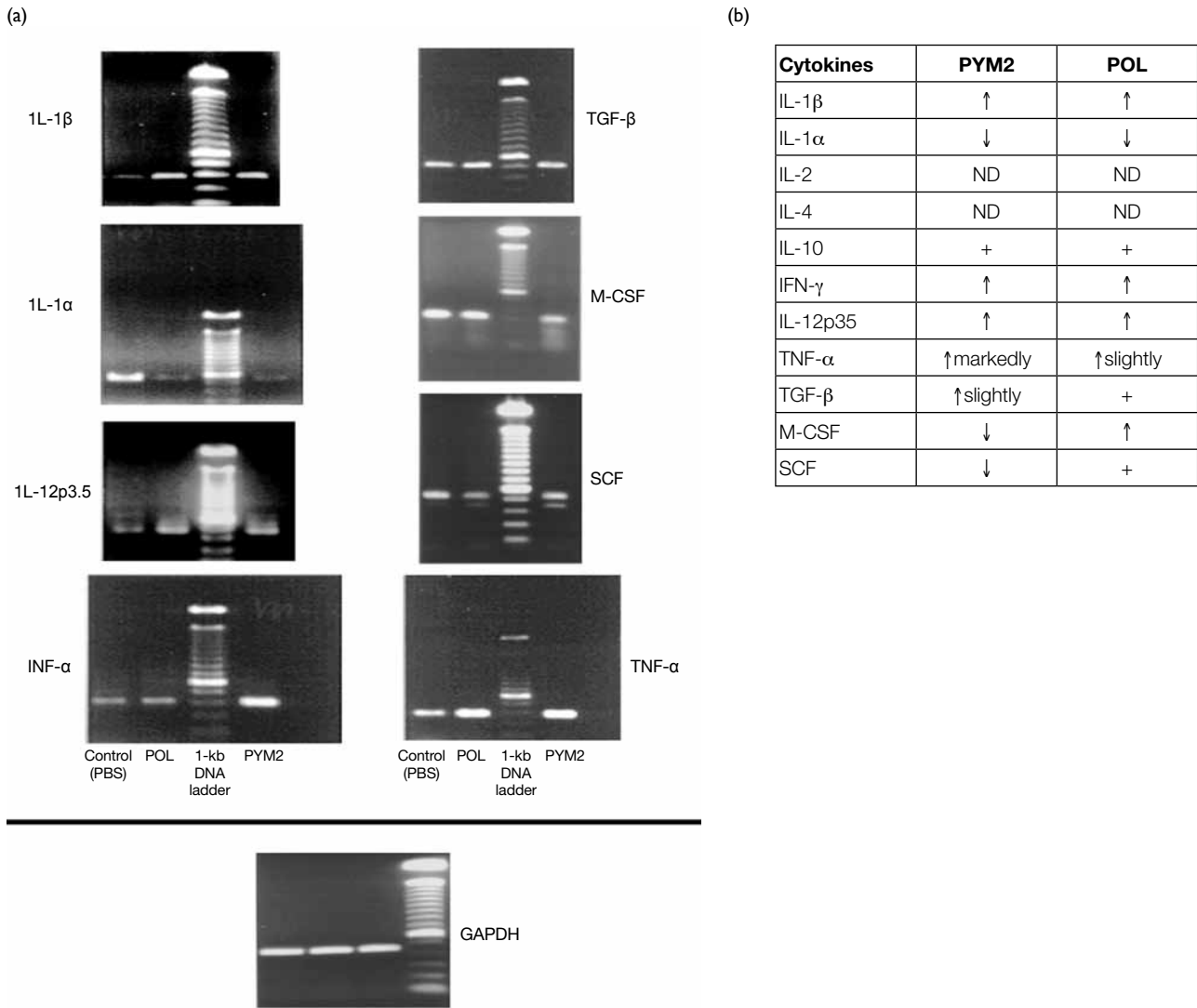
FIG 2. (a) Induction of cytokine gene expression by Pandanus amaryllifolius (PYM2) and Polygonatum odoratum (POL) in peritoneal macrophages; (b) modulation of cytokines by PYM2 and POL as in (a)

GAPDH is used as an internal standard. The proportion of densities of DNA bands is measured by a densitometer under ultraviolet light. ↑ denotes up-regulated, ↓ down-regulated, ND not detectable, + detectable but remains unchanged as compared to the control

The potency of the active antiviral proteins for modulating the immune system was evaluated. After induction of PYM2 and POL in mouse macrophages 48 hours after intraperitoneal injection of 5 mg/kg of the proteins, production and gene expression of IL-1β, IL-12p35, and TNF-α were substantially up-regulated, but TGF-β was only slightly up-regulated (Fig 2). Production of IFN-γ was more prominent in PYM2- than POL- induced macrophages. In blood serum, up-regulation of several cytokines was demonstrated. Compared with the control group (treated with only PBS), the up-regulation of IL-1β, IL-12, IFN-γ, and TNF-α was pronounced. A similar pattern appeared both in the induction by the proteins in cytokine production and gene expression in macrophages and the level of cytokines in blood serum of the mouse (Fig 2).

Discussion

Three proteins, namely PYM2, NTL, and POL, showed most activity against H1N1 and H5N1 viruses. As molecular cloning and characterisation of NTL had been extensively studied, investigation was focused on the expression of PYM2 and POL in bacteria (*E coli*). The proteins were confirmed to have significant inhibitory effects against H5N1 virus. For comparison, the soluble seed protein from Gt1/SP$_{POL}$/POL transgenic rice (obtained from another

project) was compared with purified POL for their effects on inhibiting virus infection. POL expressed in rice retains its potency against the virus. New application of herbal proteins was explored for the feasibility of rice-derived proteins against H5N1 virus and other human viruses. Further anti-viral activity assays such as plaque reduction assay should be performed using chromatographic column-purified rice protein.

The immune modulatory potency of the active antiviral substances was also evaluated for product development potential. The immunomodulatory effect of PYM2 and POL were investigated for their ability to induce production and gene expression of macrophage cytokines and the level of cytokines in blood serum of the mice after intraperitoneal injection of the test samples (PYM2 or POL or PBS as a control). The immunomodulation by PYM2 and POL on the cytokine profiles was monitored by the ELISA. The production and gene expression of IL-1β, IL-12p35, IFN-γ, and TNF-α were substantially up-regulated, but TGF-β was only slightly up-regulated. There was up-regulation of several cytokines in blood serum. Compared with the control group (treated with only PBS), the up-regulation of IL-1β, IL-12, IFN-γ, and TNF-α in mouse blood serum was prominent. This indicated that PYM2 or POL had some immunomodulatory effects in vivo, although its mechanism awaits elucidation.

Acknowledgement

References

1. To KF, Chan PK, Chan KF, et al. Pathology of fatal human infection associated with avian influenza A (H5N1) virus. J Med Virol 2001;63:242-6.
2. Hurt AC, Selleck P, Komadina N, Shaw R, Brown L, Barr IG. Susceptibility of highly pathogenic A (H5N1) avian influenza viruses to the neuraminidase inhibitors and adamantanes. Antiviral Res 2007;73:228-31.
3. Ehrhardt C, Hrincius ER, Korte V, et al. A polyphenol rich plant extract, CYSTUS052, exerts anti influenza virus activity in cell culture without toxic side effects or the tendency to induce viral resistance. Antiviral Res 2007;76:38-47.
4. Serkedjieva J, Velcheva M. In vitro anti-influenza virus activity of the pavine alkaloid (-)-thalimonine isolated from Thalictrum simplex L. Antivir Chem Chemother 2003;14:75-80.
5. O'Keefe BR, Smee DF, Turpin JA, et al. Potent anti-influenza activity of cyanovirin-N and interactions with viral hemagglutinin. Antimicrob Agents Chemother 2003;47:2518-25.

DNAzymes for treatment of dengue fever

L Baum *, KE Olson, PKS Chan, WY Lam

KEY MESSAGES

1. Dengue virus is carried by mosquitoes and afflicts 50 to 100 million people each year.

2. DNAzymes are fragments of DNA that can destroy specific sequences of RNA.

3. We have discovered two DNAzymes that can destroy the RNA of dengue virus.

4. These DNAzymes might be developed into drugs to treat infection with dengue virus.

Introduction

Dengue virus is carried by mosquitoes and can cause dengue fever, dengue haemorrhagic fever, and dengue shock syndrome, afflicting 50 to 100 million people each year.[1] The genetic material of the virus consists of RNA.[1] DNAzymes are molecules that can cut RNA at certain places. DNAzymes are pieces of DNA.

DNA and RNA are strings of units made up of bases. There are four possible bases arranged in any order to make an infinite variety of DNA or RNA molecules. DNA has two strands. Bases can fit together with other bases like jigsaw puzzle pieces: A pairing with T, and C pairing with G.

DNAzymes are shaped like the Greek letter Ω, with the loop containing a series of bases that together have a special ability to cut RNA.[2] DNAzymes can be custom-made to cut a specific piece of RNA. To do this, one chooses bases in the horizontal part of the Ω that pairs with the specific fragment of RNA. DNAzymes have been used effectively in animals.[3] DNAzymes have the potential to attack the RNA in dengue viruses.[2] Therefore, we made and tested DNAzymes that may be used to treat dengue virus infection.

Methods

This study was conducted from December 2006 to December 2007. We found 51 regions of dengue virus RNA that were the same in different strains. Within these regions, 26 good DNAzyme cutting sites were identified and 26 DNAzymes to cut these sites were made. To test the ability of each DNAzyme to cleave dengue RNA, we grew dengue virus, purified its RNA, mixed the RNA with a DNAzyme, and left the mixture for some time. To determine whether the RNA was cut, gel electrophoresis was performed to separate fragments of RNA or DNA according to their size.

Results

Two DNAzymes (A and R) displayed cleavage activity. The Figure shows the gel separating the RNA and its fragments by their sizes, and the Table lists the contents of the mixtures that were separated on each lane of the gel. Magnesium chloride ($MgCl_2$) is required for optimal cleavage by DNAzymes. Increasing the $MgCl_2$ concentration increased cleavage by both DNAzymes. Complete fragmentation of RNA was only observed with DNAzyme A with the highest tested $MgCl_2$ concentration, but even the lowest concentration had at least a partial effect. Increasing the incubation period from 30 to 60 minutes did not affect the cleavage noticeably.

Discussion

Two (8%) out of 26 DNAzymes (termed A and R) were found to cleave dengue RNA. This was comparable to that in a study showing that two out of 16 DNAzymes tested successfully cut the targeted RNA.[4] The two
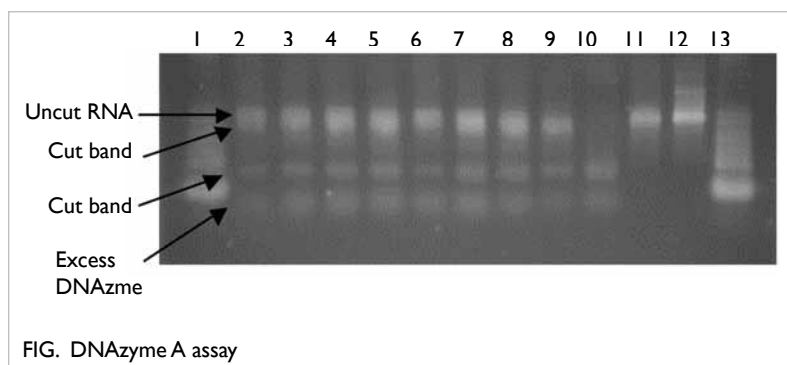

FIG. DNAzyme A assay

TABLE. DNAzyme A assay

Lane	1	2	3	4	5	6	7	8	9	10	11	12	13
RNA (relative units)	-	1	1	1	1	1	1	1	1	1	1	1	-
DNAzyme (relative units)	-	1	1	1	1	1	1	1	1	1	-	-	-
MgCl$_2$ (relative units)	-	1	2	3	4	1	2	3	4	10	2	-	-
Incubation time (min)	-	30	30	30	30	60	60	60	60	60	60	-	-

DNAzymes that target different regions of dengue viral RNA may be used simultaneously to increase the chance of cleaving each strand of viral RNA.

Several obstacles need to be overcome before DNAzyme therapy can be realised: delivery across cell membranes, metabolism, digestion of DNAzymes, and optimising inhibitory and cleavage activity. Future work should involve testing modifications to increase the activity of DNAzymes A and R in serum and cultured cells infected with dengue virus. Delivery of DNAzymes to infected cells is a challenge, for which chemical modifications may enhance entry into cells.[5] Future work should also entail measuring the speed and efficiency by which DNAzymes cut RNA. In addition, variants of DNAzymes A and R (as negative controls) should be tested to demonstrate that the activity observed is specific.

Chemical modifications of DNAzymes can improve their activity.[6] Future work may involve testing modifications to increase the activity of DNAzymes A and R in cells infected with dengue virus. After optimising conditions for treating cells and animals and after ensuring the safety of treatment, human trials may proceed. If effective in treating dengue virus infection, DNAzymes could have the potential to save thousands of lives annually. Similarly, DNAzymes could be developed to treat other viral diseases, such as hepatitis, AIDS, and pandemic influenza.

Acknowledgments

References

1. Adelman ZN, Sanchez-Vargas I, Travanty EA, et al. RNA silencing of dengue virus type 2 replication in transformed C6/36 mosquito cells transcribing an inverted-repeat RNA derived from the virus genome. J Virol 2002;76:12925-33.
2. Santoro SW, Joyce GF. A general purpose RNA-cleaving DNA enzyme. Proc Natl Acad Sci U S A 1997;94:4262-6.
3. Khachigian LM, Fahmy RG, Zhang G, Bobryshev YV, Kaniaros A. c-Jun regulates vascular smooth muscle cell growth and neointima formation after arterial injury. Inhibition by a novel DNA enzyme targeting c-Jun. J Biol Chem 2002;277:22985-91.
4. Cieslak M, Niewiarowska J, Nawrot M, Koziolkiewicz M, Stec WJ, Cierniewski CS. DNAzymes to beta 1 and beta 3 mRNA down-regulate expression of the targeted integrins and inhibit endothelial cell capillary tube formation in fibrin and matrigel. J Biol Chem 2002;277:6779-87.
5. Hashida H, Miyamoto M, Cho Y, et al. Fusion of HIV-1 Tat protein transduction domain to poly-lysine as a new DNA delivery tool. Br J Cancer 2004;90:1252-8.
6. Schubert S, Gul DC, Grunert HP, Zeichhardt H, Erdmann VA, Kurreck J. RNA cleaving '10-23' DNAzymes with enhanced stability and activity. Nucleic Acids Res 2003;31:5982-92.

Cellular enhancing and restricting factors of dengue virus egress

PG Wang *, M Kudelko, KTH Kwok, R Bruzzone, B Nal

KEY MESSAGE

Class II Arfs (Arf4 and Arf5) play a crucial role in the egress of dengue viruses.

PG Wang *, M Kudelko, KTH Kwok, R Bruzzone, B Nal

HKU-Pasteur Research Centre, 8 Sassoon Road, Hong Kong

* Principal applicant and corresponding author: peigangwang@gmail.com

Introduction

Dengue viruses of four serotypes (DV1-4) are the pathogens of dengue fever, dengue haemorrhagic fever, and dengue shock syndrome. An estimated 50 to 100 millions such cases (including 25 000 deaths) occur every year. There is no established treatment for such infections.

The life cycle of dengue viruses, like other enveloped viruses, can be divided into three stages: entry, replication, and egress. Each stage requires participation of the virus itself and/or host cells. For example, viral entry needs a cellular receptor for attachment and penetration through the lipid membrane of the host cell. The hijacking of cellular factors is a common strategy for the virus to complete its life cycle. Although such cellular factors do not assemble into newborn viral particles, they are indispensable for the viral life cycle and thus are potential targets for anti-virus therapy. If these crucial cellular factors cannot be used by the virus, viral replication can be inhibited. Therefore, identifying these crucial factors is important in the fight against the virus.

This study focuses on the late stage of the dengue virus life cycle in host cell—egress. The egress process of enveloped viruses entails assembly followed by transportation of the virus. Assembly of dengue virus occurs in the endoplasmic reticulum (ER). Nascent virions in the ER need to be transported to the Golgi apparatus, and then to the plasma membrane before they are finally released.[1] Cellular trafficking machinery, especially the secretory pathway is believed to be involved in the assembly followed by transportation of dengue virus. We aimed to identify such cellular trafficking factors involved in the egress of dengue virus.

Structurally, dengue virus particles can be divided into internal and external parts.[2] The internal part consists of capsid protein and the RNA genome, which carry viral genetic information and participate in viral replication. The external part is made up of a lipid membrane, prM and E glycoproteins, which are responsible for both viral entry and egress. During viral entry, E glycoprotein binds to cellular receptors and triggers virus-cell membrane fusion. During the secretion process, prM and E glycoproteins interact with a cellular factor along the secretory pathway. For example, the prM protein is cleaved by furin (a major processing enzyme of the secretory pathway) to form M and soluble pr proteins. Such cleavage is critical for maturation of dengue virions. prM and E glycoproteins are also essential for viral assembly occurred in ER. In the presence of capsid protein and RNA genome, prM and E proteins initiate assembly to form nascent virions, whereas in the absence of capsid protein and the RNA genome, prM and E proteins form virus-like particle (VLPs) only.[3]

Dengue VLPs are generated by glycoprotein prME in the absence of the capsid protein and RNA genome. Thus, dengue VLPs consist of the external structure of the dengue virus, but lack the viral genome and thus cannot cause infection (Fig 1). In a previous study, we developed a dengue VLP–producing stable cell line (HeLa-prME) using a codon-optimised dengue prME gene that markedly increases the expression of prME in mammalian cells.[3] The VLPs formed in the ER, and then went through the same egress pathway like dengue virus.[3] Thus, dengue VLPs can mimic the egress of fully formed virus, and therefore constitutes a safe and convenient tool to study the egress of dengue virus.[3]

Methods and results

This study was conducted from August 2008 to July 2010. To identify cellular factors that play important roles in the egress of dengue virus, HeLa-prME cells were used to screen a small interfering RNA (siRNA) library. An siRNA library screen is useful to identify interesting genes from the whole genome of the host cell or from a cluster of genes for specific functions.

Treatment with an siRNA that targets a gene can specifically deplete expression of this gene. Several cellular factors involved in replication of flaviviruses have been identified by screening the whole genome siRNA library. We screened a cellular membrane trafficking siRNA library that targets 122 cellular factors. Each of them was depleted in HeLa-prME cells by siRNA treatment, and their effects on VLPs egress was determined by measuring the amount of VLPs released into the culture medium.

After screening the siRNA library and some other cellular trafficking genes, 23 genes were noted to result in significant reduction of VLPs released, whereas 22 other genes induced a significant increase. Among the cellular factors, Arf 4 and Arf5 were the most interesting. These two factors belong to the ADP-ribosylation factor family, of which six members have been identified so far with only five expressed in humans (Arf2 has been lost). Based on amino acid sequence identity, the six Arfs were grouped into 3 classes: class I (Arf1-3), class II (Arf4, 5), and class III (Arf6).[4]

Simultaneous depletion of class II Arf (Arf4 and Arf5) blocked VLPs for all four dengue serotypes. The crucial role of class II Arfs was confirmed by a rescue experiment using an siRNA-resistant Arf5 gene. By immunofluorescence microscopy, depletion of class II Arfs did not result in VLP accumulation in any compartment downstream of the ER along the secretory pathway. Finally, depletion of class II Arfs resulted in a significant reduction of viral titre for dengue 1 and dengue 4 viruses.

Class II Arfs have been studied much less than other Arfs, and most knowledge on Arf proteins is obtained from Arf1. Arf1 protein is localised in Golgi apparatus and plays an important role in regulating the secretory pathway.[4] The transport from one compartment of the secretory pathway to the next is mediated by the formation of coated membrane vesicles that travel to and fuse with the target organelle. The formation of trafficking vesicles involves membrane curvature, which requires Arf protein. Arf1 protein is recruited to the Golgi membrane and then triggers membrane curvature and vesicle formation and trafficking.[4] Although Arf6 protein functions in different sites, its molecular mechanism is similar.[4] Arf1 protein is hijacked by viruses such as HIV and HCV for assembly or replication, whereas Arf6 protein is hijacked by the coxsackie virus or HIV for virus entry.[4] Thus, class II Arfs are similarly required for the membrane curvature during egress of the dengue virus.[4]

Notably, depletion of Arf1 by siRNA partially reduces the release of dengue VLPs in a manner different from class II Arfs. Arf 4 and Arf5 are functionally redundant during egress of the dengue virus. Our results showed that production of dengue VLPs could not be reduced by Arf4 siRNA or Arf5
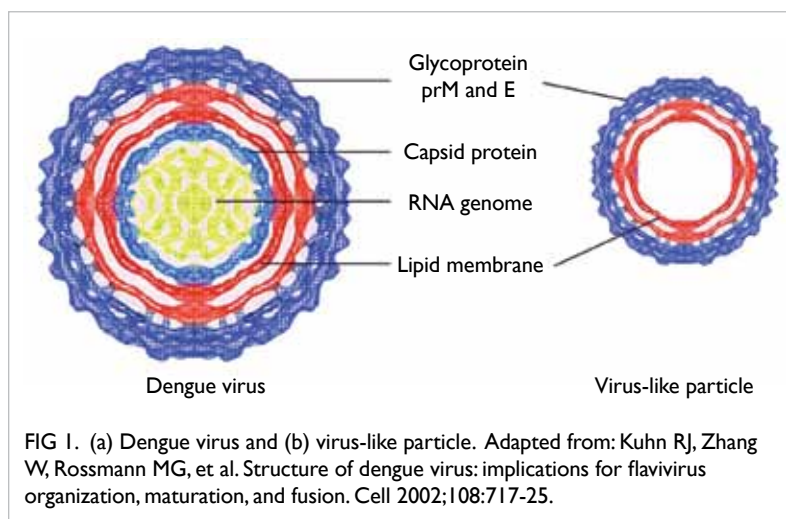

FIG 1. (a) Dengue virus and (b) virus-like particle. Adapted from: Kuhn RJ, Zhang W, Rossmann MG, et al. Structure of dengue virus: implications for flavivirus organization, maturation, and fusion. Cell 2002;108:717-25.
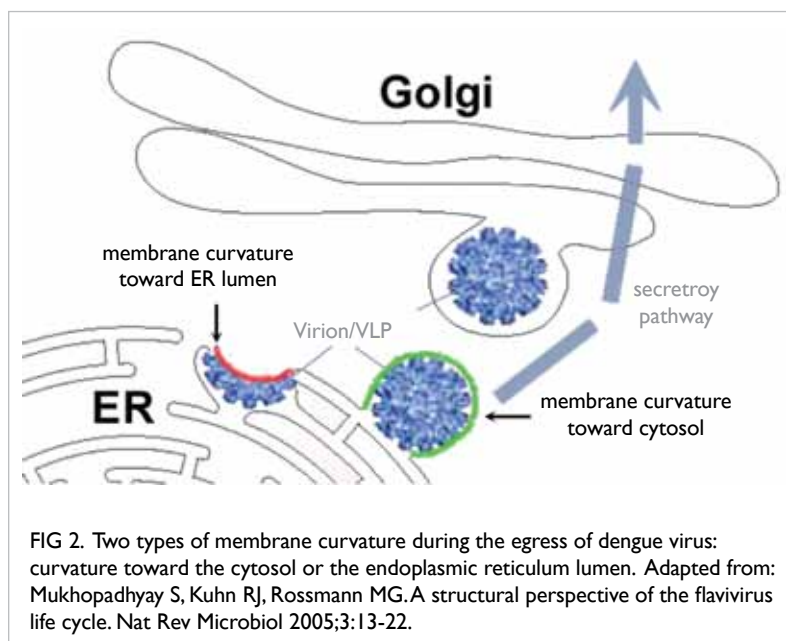

FIG 2. Two types of membrane curvature during the egress of dengue virus: curvature toward the cytosol or the endoplasmic reticulum lumen. Adapted from: Mukhopadhyay S, Kuhn RJ, Rossmann MG. A structural perspective of the flavivirus life cycle. Nat Rev Microbiol 2005;3:13-22.

siRNA alone, and a single class II Arf protein is sufficient to sustain the proper egress of dengue virus, indicating the overlapping role of Arf4 with Arf5. The functional redundancy of the two Arfs at a site is a common rule for all six Arf proteins.[5] However, such an overlap could not be observed between class II Arfs and Arf1. Simultaneous depletion of Arf1 with any member of class II Arfs did not show stronger inhibition than Arf1 alone. The effect of Arf1 on VLPs release can be explained by Arf1's role in the Golgi apparatus along the secretory pathway. Thus, class II Arfs may be required at a site other than the Golgi apparatus.

There are two types of membrane curvatures during egress of the dengue virus (Fig 2). The first is curvature towards the cytosol to form trafficking vesicles. Class II Arfs were critical for the formation of trafficking vesicle, which brings nascent virions

from ER to Golgi apparatus. The second is curvature towards the ER lumen to form nascent virions. Virus particles or VLPs are spherical membrane structure–like trafficking vesicles and their formation requires the curvature towards the ER lumen. The curved lipid membrane finally becomes a part of the nascent virion (Fig 2). Based on the evidence that class II Arfs (rather than class I Arfs) are partially colocalised with the ER marker calreticulin, and that E protein in HeLa-prME cells is mainly localised to ER, we support the second explanation that class II Arfs are recruited to the ER membrane through interaction with dengue glycoprotein prME and then facilitate membrane curvature and formation of the dengue particle.

Although the mechanism by which class II Arfs are involved remains unknown, our findings shed new light on a molecular mechanism used by dengue viruses during the late stages of their replication cycle and demonstrate a novel role for class II Arf proteins.

Acknowledgements

References

1. Mukhopadhyay S, Kuhn RJ, Rossmann MG. A structural perspective of the flavivirus life cycle. Nat Rev Microbiol 2005;3:13-22.
2. Kuhn RJ, Zhang W, Rossmann MG, et al. Structure of dengue virus: implications for flavivirus organization, maturation, and fusion. Cell 2002;108:717-25.
3. Wang PG, Kudelko M, Lo J, et al. Efficient assembly and secretion of recombinant subviral particles of the four dengue serotypes using native prM and E proteins. PLoS One 2009;4:e8325.
4. D'Souza-Schorey C, Chavrier P. ARF proteins: roles in membrane traffic and beyond. Nat Rev Mol Cell Biol 2006;7:347-58.
5. Volpicelli-Daley LA, Li Y, Zhang CJ, Kahn RA. Isoform-selective effects of the depletion of ADP-ribosylation factors 1-5 on membrane traffic. Mol Biol Cell 2005;16:4495-508.

AUTHOR INDEX